0026-895X/09/7602-275–289$20.00
MOLECULAR PHARMACOLOGY
Vol. 76, No. 2
54783/3494193
Mol Pharmacol 76:275–289, 2009
Printed in U.S.A.

Five Amino Acids in the Innermost Cavity of the Substrate Binding Cleft of Organic Cation Transporter 1 Interact with Extracellular and Intracellular Corticosterone

Christopher Volk, Valentin Gorboulev, Alexander Kotzsch, Thomas D. Müller, and Hermann Koepsell

Institute of Anatomy and Cell Biology (C.V., V.G., H.K.) and Department of Molecular Plant Physiology and Biophysics, Julius-von-Sachs Institute (A.K., T.D.M.), Universität Würzburg, Würzburg, Germany

Received January 15, 2009; accepted May 12, 2009

ABSTRACT

We have shown previously that Leu447 and Gln448 in the transmembrane helix (TMH) 10 of rat organic cation transporter rOCT1 are critical for inhibition of cation uptake by corticosterone. Here, we tested whether the affinity of corticosterone is different when applied from the extracellular or intracellular side. The affinity of corticosterone was determined by measuring the inhibition of currents induced by tetraethylammonium$^+$ (TEA^+) in *Xenopus laevis* oocytes expressing rOCT1. Either corticosterone and TEA^+ were added to the bath simultaneously or the oocytes were preincubated with corticosterone, washed, and TEA^+-induced currents were determined subsequently. In mutant L447Y, K_i values for extracellular and intracellular corticosterone were decreased, whereas in mutant Q448E, only the K_i for intracellular corticosterone was changed. Modeling of the interaction of corticosterone with rOCT1 in the inward- or outward-facing conformation predicted direct binding to Leu447, Phe160 (TMH2), Trp218 (TMH4), Arg440 (TMH10), and Asp475 (TM11) from both sides. In mutant F160A, affinities for extracellular and intracellular corticosterone were increased, whereas maximal inhibition was reduced in W218F and R440K. In stably transfected epithelial cells, the affinities for inhibition of 1-methyl-4-phenyl-pyridinium$^+$ (MPP^+) uptake by extracellular and intracellular corticosterone were decreased when Asp475 was replaced by glutamate. In mutants F160A, W218Y, R440K, and L447F, the affinities for MPP^+ uptake were changed, and in mutant D475E, the affinity for TEA^+ uptake was changed. The data suggest that Phe160, Trp218, Arg440, Leu447, and Asp475 are located within an innermost cavity of the binding cleft that is alternatingly exposed to the extracellular or intracellular side during substrate transport.

Polyspecific organic cation transporters (OCTs) of the *SLC22* family play important roles in the elimination, distribution, and homeostasis of drugs. In addition, they are involved in the reuptake of neurotransmitters into neurons and release of acetylcholine during non-neuronal cholinergic reactions (Lips et al., 2005; Koepsell et al., 2007; Reitman and Schadt, 2007). Three OCT subtypes with overlapping substrate specificities and tissue distributions have been identified (Koepsell et al., 2007). OCT1, OCT2, and OCT3 are polyspecific facilitated diffusion systems that are able to translocate organic cations in both directions across the plasma membrane. However, it remains unclear how OCTs recognize substrates and inhibitors exhibiting different chemical structures and how substrate translocation is achieved. Extensive mutagenesis experiments performed in rat OCT1 (rOCT1) revealed that seven amino acids localized in the 4th, 10th, and 11th transmembrane helices (TMH) are critical for substrate and inhibitor specificity (Gorboulev et al., 1999, 2005; Popp et al., 2005). Modeling of the rOCT1 structures using the inward-facing structure of lactose permease (LacY) from *Escherichia coli* (Abramson et al., 2003; Popp et al., 2005) suggested that the residues critical for substrate affinity are localized within a large inward-open cleft and are accessible from the solvent space. In analogy to the conformational changes of the permease LacY via the alternating access mechanism model—which has been experimentally demonstrated for LacY (Smirnova et al., 2006; Kaback et al., 2007; Majumdar et al., 2007)—we have also modeled the outward-facing conformation of rOCT1 with the

This work was supported by the Deutsche Forschungsgemeinschaft Grant SFB 487/A4.
Article, publication date, and citation information can be found at http://molpharm.aspetjournals.org.
doi:10.1124/mol.109.054783.

ABBREVIATIONS: OCT, organic cation transporter; r, rat; TMH, transmembrane helix; TEA, tetraethylammonium; MPP, 1-methyl-4-phenylpyridinium; MOPS, 3-(*N*-morpholino)propanesulfonic acid; TBuA, tetrabutylammonium; HEK, human embryonic kidney; PBS, phosphate-buffered saline; LacY, lactose permease from *Escherichia coli*; ANOVA, analysis of variance.

binding cleft opened to the extracellular space (Gorbunov et al., 2008). So far, two observations support the hypothesis that OCTs operate via an alternating access mechanism model similar to that of LacY. First, measuring interactions of nontransported inhibitors applied from the extracellular or intracellular side of the plasma membrane provides evidence that the substrate-binding region of rat OCT2 (rOCT2) is accessible from the extracellular and intracellular sides (Volk et al., 2003). Second, we demonstrated that mutations in modeled contact regions between TMH2 and TMH11, which interact in the inward-facing model and are detached in the outward-facing model, may partially inhibit transport activity (Gorbunov et al., 2008).

We previously identified two residues that are responsible for increased affinity of corticosterone to inhibit uptake of tetraethylammonium$^+$ (TEA^+) by rOCT2 compared with rOCT1 (Gorboulev et al., 2005). Upon replacement of Leu447 and Gln448 in TMH10 of rOCT1 by the corresponding amino acids of rOCT2 [mutant rOCT1(L447Y,Q448E)], the IC_{50} value for inhibition of [^{14}C]TEA^+ uptake by corticosterone decreased to the value observed in rOCT2. The Michaelis-Menten constant (K_m) for 1-methyl-4-phenylpyridinium$^+$ (MPP^+) uptake was also decreased in rOCT1(L447Y,Q448E), suggesting that Leu447 and/or Gln448 are located within the substrate binding region. The K_i values for corticosterone-mediated inhibition of TEA^+ uptake were determined using an incubation time of 30 min. Because corticosterone permeates the plasma membrane passively during this period (Arndt et al., 2001), we cannot distinguish whether the mutations increase the affinity for corticosterone from the extracellular side, from the intracellular side, or from both sides of the plasma membrane.

The structure models of the inward- and outward-facing conformations of rOCT1 (Popp et al., 2005; Gorbunov et al., 2008) suggested that Leu447 may contribute to the outward- and inward-facing cleft, whereas Gln448 seemed to be accessible only in the inward open cleft. To determine whether residues that contribute to both the outward- and inward-facing substrate-binding regions can be identified experimentally, we investigated whether the mutations L447Y and Q448E alter the affinity for corticosterone, which was applied to the extracellular or intracellular side of the plasma membrane. From docking analysis of corticosterone in the outward- and inward-facing binding clefts of rOCT1, we could identify additional amino acids that possibly interact with corticosterone and were thus tested by mutagenesis.

Here we present evidence that the residues Phe160 (TMH2), Trp218 (TMH4), Arg440 (TMH10), Leu447 (TMH10), and Asp475 (TMH11) are located in the innermost cavities of the outward-facing as well as the inward-facing substrate binding clefts. All these residues participate in the binding of corticosterone on either side of the plasma membrane and are critical for the binding affinity of MPP^+ or TEA^+.

Materials and Methods

Materials. [^{14}C]TEA^+ (1.9 GBq/mmol) and [^{3}H]MPP^+ (3.1 TBq/mmol) were obtained from Biotrend (Köln, Germany). All other chemicals were obtained as described previously (Arndt et al., 2001; Volk et al., 2003).

Site-Directed Mutagenesis. Point mutations were introduced into rOCT1 by polymerase chain reaction, applying the overlap extension method as described previously (Ho et al., 1989; Gorboulev et al., 2005; Popp et al., 2005). The cloned fragments were sequenced to confirm the presence of the desired mutations.

Expression of rOCT1 and Mutants in *Xenopus laevis* Oocytes. *X. laevis* oocytes were prepared as described previously (Arndt et al., 2001) and stored in Ori buffer (5 mM MOPS, 100 mM NaCl, 3 mM KCl, 2 mM $CaCl_2$, and 1 mM $MgCl_2$, adjusted to pH 7.4 using NaOH) supplemented with 50 mg/l gentamicin. cRNA (10 ng) encoding for wild-type rOCT1 or the mutants were injected in a volume of 50 nl of H_2O into single oocytes. Oocytes were then stored for 3 to 5 days in Ori buffer at 16°C. Noninjected oocytes from the respective batch served as controls.

Electrophysiology. Two-electrode voltage-clamp measurements were performed as described previously (Nagel et al., 1997; Volk et al., 2003). Oocytes were superfused continuously with Ori buffer at room temperature (~2 ml/min) and routinely clamped to a holding potential of −50 mV using an amplifier (OC 725; Warner Instruments, Hamden, CT). Apparent K_m values for TEA^+ were determined by superfusing voltage-clamped oocytes with increasing TEA^+ concentrations and recording the induced inward currents.

Inhibition of TEA^+-Induced Currents by Tetrabutylammonium$^+$ or Corticosterone. To measure the inhibition of TEA^+-induced inward currents due to binding of tetrabutylammonium$^+$ ($TBuA^+$) or corticosterone to rOCT1 from the extracellular side, oocytes were superfused for 45 s with Ori buffer containing TEA^+, TEA^+ plus $TBuA^+$, or TEA^+ plus corticosterone. The concentration dependence for inhibition of rOCT1 by $TBuA^+$ or corticosterone was determined by starting the superfusion with the lowest inhibitor concentration. After each superfusion period, the oocytes were washed for 1 min with Ori buffer. To measure inhibition of TEA^+-induced inward currents that was due to corticosterone binding from the intracellular side, oocytes were clamped to −50 mV, equilibrated for 10 min with corticosterone and washed for 1 min with Ori buffer. Then TEA^+-induced inward currents were measured during a 45-s superfusion period with TEA^+. The 10-min equilibration periods in the presence of corticosterone were started at the lowest corticosterone concentration.

Control experiments showed that the cytosolic corticosterone concentration required for inhibition of rOCT1 from the intracellular side is reached after 10 min of incubation (equilibration control) and that the access of corticosterone to the extracellular surface after 45-s incubation with corticosterone from the extracellular side as well as 10-min preincubation with corticosterone can be eliminated with a 1-min wash using Ori buffer (wash controls). The equilibration control was performed with the mutant rOCT1(C451M, Q448E), which has a much higher affinity for corticosterone applied to the intracellular side as when applied from the extracellular side (Table 1). When oocytes expressing rOCT1(C451M, Q448E) were incubated for 10 or 30 min with 4.6 μM corticosterone, virtually identical inward currents were obtained after superfusion with 0.2 mM TEA^+. The currents amounted to 52 ± 4% (10-min incubation, $n = 4$) and 48 ± 4% (30-min incubation, $n = 4$ each) of the currents obtained without corticosterone pretreatment. Because 4.6 μM corticosterone is the half-maximal concentration [$IC_{50(cort.)}$] for inhibition of rOCT1(C451M, Q448E) from the intracellular side and the $IC_{50(cort)}$ from extracellular is 10-fold higher, we conclude that the cytosolic concentration of corticosterone is equilibrated after 10-min incubation. The wash controls were performed with rOCT1(C451M), which exhibits a higher affinity for corticosterone applied from extracellular than from the intracellular side (Table 1). In oocytes expressing rOCT1(C451M), current induced by superfusion with 0.2 mM TEA^+ was inhibited by 50 ± 3% ($n = 4$) when 45-s superfusion with TEA^+ was performed in the presence of 49 μM corticosterone, a concentration that represents the $IC_{50(cort.)}$ from extracellular. The inhibition was virtually abolished (2 ± 2%, $n = 4$) after the oocytes had been washed for 1 min with Ori buffer, indicating that extracellular corticosterone as well as corticosterone that had entered the plasma membrane during the 45-s superfusion was removed. To demon-

strate that intracellular corticosterone or corticosterone inside the plasma membrane does not get access to the extracellular side during electrical measurements of washed oocytes that had been preincubated with corticosterone, we incubated oocytes expressing rOCT1(C451M) for 10 min with 49 μM corticosterone, washed them for 1 min with Ori buffer, and measured the current induced by superfusion with 0.2 mM TEA^+. The TEA^+-induced current amounted to 15 ± 3% (n = 4) of the current obtained without corticosterone pretreatment. Because this inhibition is due to inhibition from intracellular [$IC_{50(cort.)}$ from intracellular = 132 μM; Table 1], we conclude that intracellular corticosterone or corticosterone within the plasma membrane does not get significant access to the extracellular side of the transporter.

Tracer Uptake Measurements. *X. laevis* oocytes expressing rOCT1 were incubated for 15 min at room temperature in Ori buffer containing [^{14}C]TEA^+ in the presence of different concentrations of MPP^+. Subsequently, the oocytes were washed three times with ice-cold Ori buffer, solubilized by using 5% SDS solution, and the intracellular radioactivity was analyzed by liquid scintillation counting using a Packard TriCarb 1600 counter (PerkinElmer Life and Analytical Sciences, Waltham, MA).

[^{3}H]MPP^+ uptake into human embryonic kidney (HEK) 293 cells stably transfected with wild-type rOCT1 or rOCT1(D475E) was measured as described previously (Mehrens et al., 2000; Minuesa et al., 2009). Cells were detached from culture plates by incubation with Ca^{2+}- and Mg^{2+}-free PBS and suspended in PBS containing 0.5 mM $MgCl_2$ and 1 mM $CaCl_2$ (transport PBS). To measure inhibition of [^{3}H]MPP^+ uptake by extracellular corticosterone, 90 μl of cells were placed at the bottom of 2-ml tubes and incubated for 40 s at 37°C. Ten microliters of transport PBS containing 0.13 μM [^{3}H]MPP^+ plus different concentrations of corticosterone were placed on the inner wall of the tube above the cell suspension. Uptake was started by vortexing the tube and stopped after 1 s by adding 1 ml of ice-cold transport PBS containing 100 μM quinine (stop solution). To measure inhibition of [^{3}H]MPP^+ (0.013 μM) uptake by intracellular corticosterone, the cells were preincubated for 10 min at 37°C in transport PBS containing different concentrations of corticosterone. Twenty microliters of the preincubated cells were placed at the inner walls of 2-ml tubes that were preloaded with 300 μl of transport PBS (37°C) containing [^{3}H]MPP^+ (0.013 μM). Uptake was started by vortexing and stopped by adding ice-cold stop solution. Cells were spun down, washed with stop solution, solubilized with 4 M guanidine thiocyanate, and analyzed for radioactivity by liquid scintillation counting. Performing control experiments with rOCT1 mutants with an approximately 10-fold lower affinity for intracellular versus extracellular corticosterone, we verified that the corticosterone concentration at the outward-facing transporter was reduced effectively when cells that were preincubated with corticosterone were diluted in transport buffer without corticosterone.

Simulation of the Interaction of Corticosterone and $TBuA^+$ with rOCT1. SYBYL software (ver. 7.1; Tripos Inc., St. Louis, MO), including the force field software MMFF94s, was used throughout the simulations. For docking of corticosterone, a template coordinate set was obtained from the Protein Data Bank Ligand Expo database (http://ligand-depot.rcsb.org); for $TBuA^+$, the coordinates were obtained from the Heterocompound Information Centre–Uppsala (HIC-up; http://xray.bmc.uu.se/hicup). Hydrogen atoms were attached to all heavy atoms, and the resulting structure was subsequently energy-minimized, employing a conjugate gradient algorithm. Previously established homology models of the inward- and outward-facing conformations of rOCT1 were used for docking simulations. The inward-facing conformation was built on the basis of the crystal structure of LacY (Abramson et al., 2003; Popp et al., 2005). A model of the outward-facing conformation of rOCT1 was constructed as described recently (Gorbunov et al., 2008). In essence, a rigid-body movement of the first six helices (N-terminal domain) with respect to the last six helices (C-terminal domain) was performed in analogy to the model proposed for LacY, allowing some intrahelical motions and drifting of individual domains. For LacY, this helix rearrangement has been proposed, modeled, and demonstrated experimentally (Abramson et al., 2003; Ermolova et al., 2006; Holyoake and Sansom, 2007; Kaback et al., 2007; Smirnova et al., 2007). The structure models of the inward- and outward-facing conformations of rOCT1 were complemented with hydrogens and partial charges were assigned using the AMBER7 FF02 force field.

Docking of corticosterone to the outward- and inward-facing conformation of rOCT1 and $TBuA^+$ to the outward-facing conformation were performed using the FlexX module of SYBYL 7.1 software. For simulations, the side chains of lysine residues were protonated and the carboxylate groups of aspartic and glutamic acids were ionized, whereas cysteine residues were treated as neutral. Flexible docking of corticosterone and $TBuA^+$ was performed with FlexX (Rarey et al.,

TABLE 1

Effects of various mutations in rOCT1 on affinities of corticosterone from the extracellular or intracellular side of the plasma membrane

Wild-type rOCT1 or rOCT1 with the indicated mutations were expressed in oocytes. Inhibition of currents induced by superfusion with 0.2 or 2 mM TEA^+ by extracellular or intracellular corticosterone was measured as in Figs. 2 and 4. The Hill equation was fitted to inhibition curves of individual oocytes and IC_{50} values were calculated. Mean IC_{50} values ± S.E.M. are shown. The numbers of measured oocytes are presented in parentheses. The ratios between the mean IC_{50} values measured with 2 mM TEA^+ and 0.2 mM TEA^+ [$f_{(part.compet.)}$] were used to calculate the K_i values from the IC_{50} value obtained with 0.2 mM TEA^+. The K_i value in parentheses was calculated assuming competitive inhibition.

Inhibition	Wild type	C451M	C451M, L447Y	C451M, Q448E	C451M, L447Y Q448E	C451M, F160A	C451M, Y222F	C451M, W218Y	C451M, R440K
Extracellular									
IC_{50}	66 ± 17	49 ± 5	11 ± 1.2***	48 ± 10	8.1 ± 0.8**	13 ± 1**	101 ± 7***	333 ± 42***	112 ± 15***
(0.2 mM TEA)	(3)	(11)	(8)	(6)	(4)	(5)	(5)	(4)	(6)
IC_{50}	257 ± 90	232 ± 46	38 ± 10	191 ± 58	34 ± 11	32 ± 8	417 ± 174	N.D.	588 ± 124*
(2 mM TEA)	(4)	(9)	(7)	(5)	(8)	(3)	(5)	M.I.D.(3)	(4)
$f_{(part.compet.)}$	3.89	4.73	3.45	3.98	4.20	2.50†	4.13		4.63
K_i	27.8 ± 7.2	18.4 ± 1.9	5 ± 0.5***	20 ± 4.2	3.3 ± 0.3**	6.9 ± 1.8*	26.2 ± 1.7	(93.3 ± 11.8)***	40.4 ± 5.3**
Intracellular									
IC_{50}		132 ± 34	28 ± 4*	4.6 ± 0.7**		32 ± 8*	183 ± 41	N.D.	124 ± 33
(0.2 mM TEA)		(5)	(4)	(5)		(4)	(3)	M.I.D. (5)	(5)
IC_{50}	335 ± 13	315 ± 58	25 ± 3**	9.2 ± 1.8**		78 ± 20*	502 ± 108	N.D.	N.D.
(2 mM TEA)	(3)	(7)	(6)	(4)		(4)	(5)	M.I.D.(4)	M.I.D. (5)
$f_{(part.compet.)}$		2.63	0.89†	2.00		2.44	2.74		
K_i		71 ± 19‡	28 ± 4*‡	2.7 ± 0.4**‡		18 ± 4*‡	69 ± 15‡		

N.D., not determined; M.I.D., maximum inhibition decreased.
* $P < 0.05$, ANOVA with Tukey test, difference compared with rOCT1(C451M).
** $P < 0.01$, ANOVA with Tukey test, difference compared with rOCT1(C451M).
*** $P < 0.001$, ANOVA with Tukey test, difference compared with rOCT1(C451M).
† $P < 0.01$, Student's t test, difference to rOCT1(C451M).
‡ $P < 0.001$, Student's t test, difference to inhibition from extracellular.

1996), with the place particles option selected (Rarey et al., 1999). Two rounds of simulations were performed. In the first round, docking hits of the corticosterone or $TBuA^+$ molecule were accepted at any site in the interior cleft of the inward- and/or outward-facing conformations of OCT1, and the results were sorted according to their docking energies using the corresponding total FlexX-Scores (calculated free binding energy in kilojoules per mole). The docking simulations for corticosterone in the first round were consistent with our mutagenesis data showing that Leu447 is critical for the affinity of corticosterone in the outward-facing as well as in the inward-facing rOCT1 conformations. The majority of the docking results suggested an additional interaction of corticosterone with residues Phe160 and/or Tyr222. Additional mutagenesis experiments with these two residues revealed that the affinities of corticosterone to both the outward- and inward-facing conformations of rOCT1 were increased when Phe160 was replaced by alanine, whereas replacement of Tyr222 by phenylalanine did not change the affinity of corticosterone. We therefore performed a second docking simulation using more stringent docking site restraints around residues Leu447 and Phe160. A radius of 5 Å around each of the residues was defined to allow docked molecules to be selected.

The docking simulations for $TBuA^+$ to the outward-facing conformation in the first round indicated several putative interaction sites, including a site close to Asp475. Because the affinity of $TBuA^+$ to rOCT1 is increased when Asp475 is replaced by glutamate (Gorboulev et al., 1999), we performed a second round of simulation defining a radius of 6.5 Å around Asp475 in which docking of $TBuA^+$ was allowed.

Calculations and Statistics. All electrophysiological measurements were performed with oocytes from at least three different batches. IC_{50} values for inhibition by corticosterone or $TBuA^+$ of currents induced by superfusion with TEA^+ were calculated by fitting the Hill equation allowing adjustment to different degrees of maximal inhibition. Fitting was performed to measurements with individual oocytes (for statistic comparison) and to compiled data sets (for figures). Competition between TEA^+ and corticosterone or $TBuA^+$ was tested by checking whether the IC_{50} values measured at 0.2 mM and 2 mM TEA^+ reveal the same K_i value when competition is assumed using the following equation: $K_{i(compet.)} = IC_{50}/[1 + S/K_{m(TEA)}]$. S represents the employed concentration of TEA^+, and $K_{m(TEA)}$ is the mean value of 75 μM obtained for TEA^+-induced currents in wild-type rOCT1 and employed mutants. Competitive inhibition predicts that the IC_{50} values measured with 2 and 0.2 mM

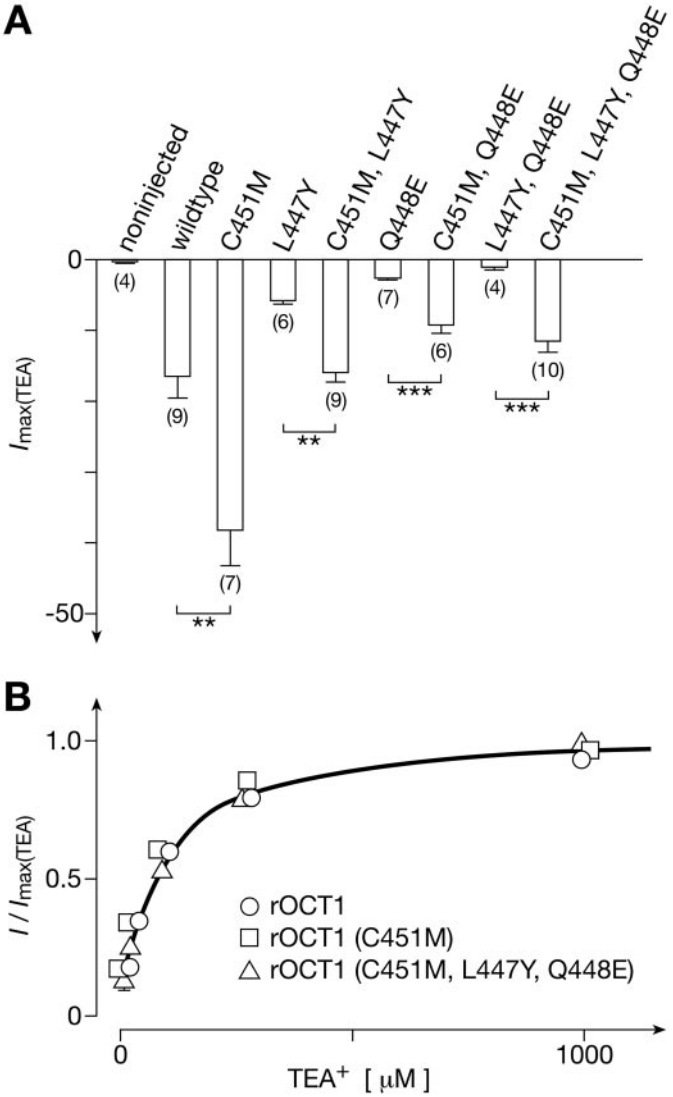

Fig. 1. Comparison of TEA^+-induced currents in wild-type rOCT1 and mutants. Noninjected oocytes or cRNA injected oocytes were incubated for 3 to 5 days, clamped to −50 mV, superfused with TEA^+, and currents induced by various concentrations of TEA^+ were measured. A, maximal currents induced by TEA^+ [$I_{max(TEA)}$]. $I_{max(TEA)}$ values were measured by superfusion of oocytes with 2 mM TEA^+. Mean values ± S.E.M are shown, and number of analyzed oocytes is indicated in parentheses. ** $P < 0.01$; ***, $P < 0.001$. B, examples for measured concentration activation curves. The Michaelis-Menten equation has been fitted to the data.

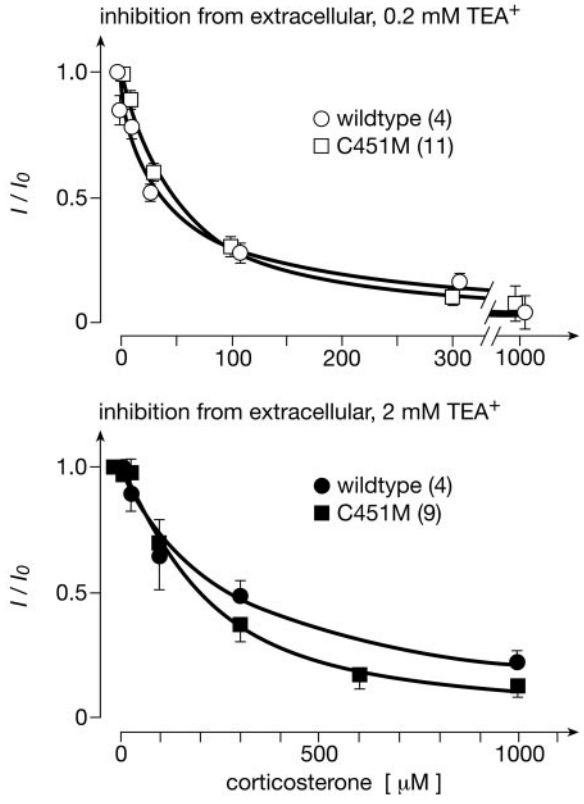

Fig. 2. Inhibition of TEA^+-induced currents mediated by wild-type rOCT1 and mutant rOCT1(C451M) by extracellular corticosterone. Oocytes expressing rOCT1 wild-type or rOCT1(C451M) were clamped to −50 mV and superfused with 45-s pulses of Ori buffer containing 0.2 mM TEA^+ plus various concentrations of corticosterone or 2 mM TEA^+ plus corticosterone. Each pulse with TEA^+ was followed by short wash with Ori buffer. Currents (I) were normalized to currents measured in the absence of corticosterone (I_0), and mean values ± S.E.M are shown. The number of analyzed oocytes is indicated in parentheses. The Hill equation was fitted to compiled data sets. The data show that the affinity of extracellular corticosterone to rOCT1 was not changed significantly after exchange of Cys451 by methionine.

TEA^+ are 28.4 and 3.74 times higher, respectively, than the calculated K_i value and that IC_{50} values measured with 2 mM TEA^+ are 7.59 times higher [$f_{(compet.)}$] compared with the values obtained with 0.2 mM TEA^+. In some experiments the observed factors between the IC_{50} values at 2 and 0.2 mM TEA^+ were smaller, indicating partial competition [$f_{(part.compet.)}$]. In the case of partial competition, we estimated the K_i values from the IC_{50} values measured with 0.2 mM TEA^+ according to the following equation: $K_{i(part.compet.)} = IC_{50}/\{1 + [S \cdot f_{(part.compet.)}]/[K_{m(TEA)} \cdot f_{(compet.)}]\}$. For example, when corticosterone was applied from the extracellular side of oocytes expressing wild-type rOCT1, the IC_{50} value measured with 2 mM TEA^+ was 3.89 times higher than those measured with 0.2 mM TEA^+ [$f_{(part.compet.)}$], and the K_i value was estimated by dividing the IC_{50} value by 2.37 (divider in the last equation).

In tracer uptake measurements with oocytes, uptake rates were calculated from 7 to 10 oocytes for each data point. Apparent K_m. values for [^{3}H]MPP^+ uptake and $I_{(0.5TEA)}$ values for activation of TEA^+-induced currents were calculated by fitting the Michaelis-Menten equation to the data, whereas IC_{50} values for inhibition of [^{14}C]TEA^+ uptake by MPP^+ were calculated using the Hill equation. In the figures, means of 4 to 10 individual experiments from at least three different batches of oocytes are presented. Measuring the inhibition of MPP^+ uptake by corticosterone in HEK293 cells, seven corticosterone concentrations were tested in three independent experiments. In each experiment and data point, four uptake measurements were performed. The IC_{50} values were determined by fitting the Hill equation to the data. Because 0.013 μM MPP^+ is far below the K_m value for MPP^+, the IC_{50} values are virtually identical to the K_i values.

Data are presented as means ± S.E.M. One way analysis of variance with post hoc Tukey test was employed to evaluate differences using Prism 4.0 (GraphPad Software Inc., San Diego, CA). P values < 0.05 were considered to be statistically significant.

Results

The Mutation C451M in rOCT1 Increases TEA^+-Induced Currents but Does Not Alter Affinity. [^{14}C]TEA^+ uptake measurements in oocytes expressing rOCT1 showed that the affinity of corticosterone was increased when Leu447 and Gln448 in TMH10 of rOCT1 were replaced by tyrosine or glutamic acid, respectively (Gorboulev et al., 2005). To determine whether these mutations alter the affinity of corticosterone from the extracellular side of the plasma membrane, we measured short-term effects of corticosterone on TEA^+-induced currents. The currents after superfusion with 2 mM TEA^+ (−50 mV) were three to eight times smaller in the mutants compared with wild-type rOCT1 (Fig. 1A, currents: wild type > L447Y > Q448E > L447Y,Q448E) and did not allow to determine reliable concentration inhibition

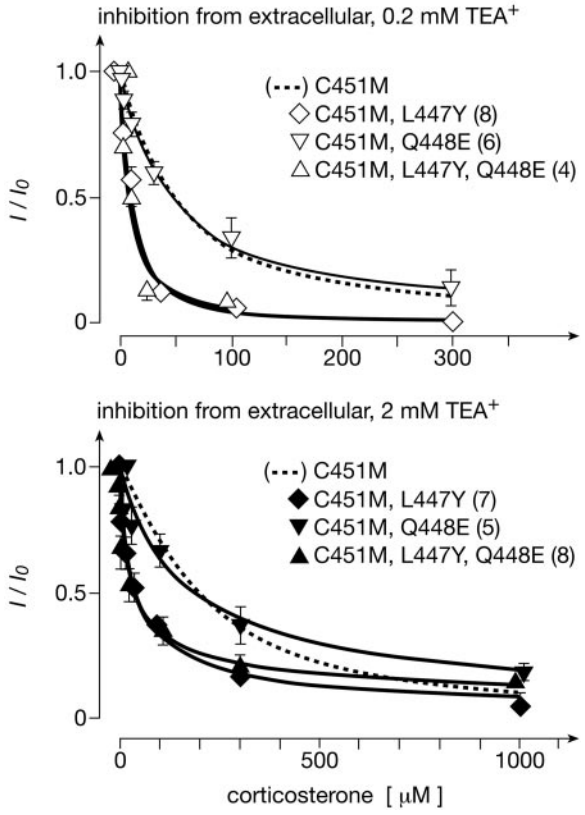

Fig. 3. Effects of mutations in positions 447 and/or 448 of rOCT1 on inhibition of TEA^+-induced currents by extracellular corticosterone. Oocytes expressing rOCT1(C451M, L447Y), rOCT1(C451M,Q448E) or rOCT1(C451M,L447Y,Q448E) were clamped to −50 mV and superfused with 45-s pulses of Ori buffer containing 0.2 mM TEA^+ plus various concentrations of corticosterone or 2 mM TEA^+ plus corticosterone. Currents (I) were normalized to currents in the absence of corticosterone (I_0). Mean values ± S.E.M with numbers of analyzed oocytes in parentheses are shown. The curves were obtained by fitting the Hill equation to compiled data sets. The experiments indicate that the affinity of extracellular corticosterone was increased after replacement of Leu447 by tyrosine.

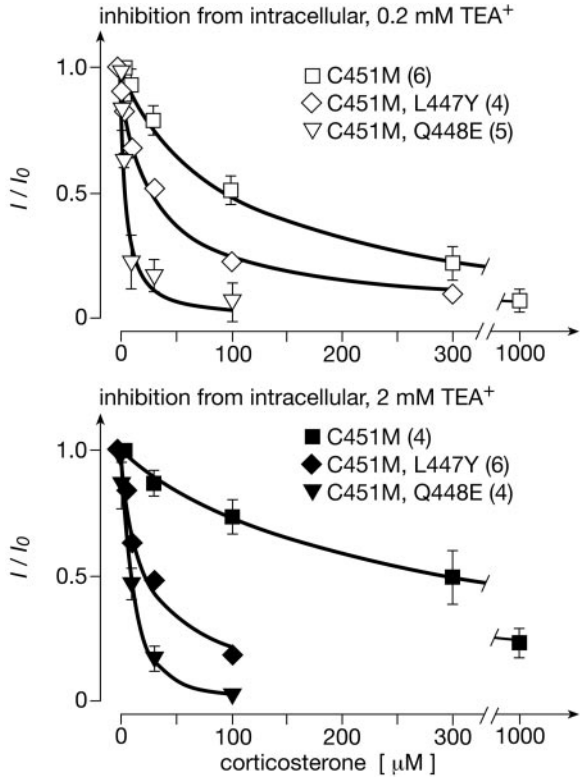

Fig. 4. Effects of mutations in positions 447 or 448 of rOCT1 on inhibition of TEA^+-induced currents by intracellular corticosterone. Mutants rOCT1(C451M), rOCT1(C451M,L447Y) or rOCT1(C451M,Q448E) were expressed in oocytes. Oocytes were clamped to −50 mV and incubated for 10 min with Ori buffer containing corticosterone. Oocytes were washed with Ori buffer, and currents induced by superfusion with Ori buffer containing 0.2 mM or 2 mM TEA^+ were measured. Currents (I) were normalized to currents in oocytes that were not preincubated with corticosterone (I_0). Mean values ± S.E.M are shown, and numbers of analyzed oocytes are indicated in parentheses. The curves were obtained by fitting the Hill equation to compiled data sets. The data show that the affinity of intracellular corticosterone was increased after replacement of Leu447 by tyrosine and of Gln448 by glutamic acid.

curves. To overcome this technical obstacle, we made use of our recent observation that I_{max} values for cation-induced currents by rOCT1 are increased when Cys451 is replaced by methionine (Sturm et al., 2007) and introduced this point mutation in the mutants with increased sensitivity to corticosterone. TEA^+-induced currents were increased as expected (Fig. 1A).

Previously, we observed that the choline concentration inducing half-maximal currents [$I_{0.5(choline)}$] in rOCT1(C451M) was increased when Cys322 was replaced with serine, whereas the same mutation in wild-type background showed no effect (Sturm et al., 2007). To test for effects of rOCT1(C451M) background, we measured the half-maximal concentrations for TEA^+ currents [$I_{0.5(TEA)}$] in oocytes expressing rOCT1, rOCT1(C451M), rOCT1(C451M,L447Y), rOCT1(C451M,Q448E), or rOCT1(C451M,L447Y,Q448E). Previous [^{14}C]TEA^+ uptake measurements showed that the apparent $K_{m(TEA)}$ values as well as the K_i values for TEA^+ inhibition of TEA^+ uptake were not significantly different in rOCT1(L447Y,Q448E) versus rOCT1 (Gorboulev et al., 2005). Likewise, we observed no effects of mutations C451M, L447Y, and/or Q448E on half-maximal activation of TEA^+-induced currents at −50 mV [$I_{0.5(TEA)}$]. The $I_{0.5(TEA)}$ values were as follows: rOCT1, 65 ± 16 μM; rOCT1(C451M), 65 ± 18 μM; rOCT1(C451M,L447Y), 82 ± 16 μM; rOCT1(C451M,Q448E), 57 ± 22 μM; and rOCT1(C451M, L447Y,Q448E), 98 ± 42 μM (n = 5–7 each; for examples, see Fig. 1B). These data suggest that mutations C451M, L447Y, and Q448E are not critical for low-affinity binding of TEA^+ to rOCT1 (Gorbunov et al., 2008).

Inhibition of rOCT1 and Mutants by Extracellular Corticosterone. We have observed that corticosterone inhibited uptake of 10 μM [^{14}C]TEA^+ in oocytes expressing wild-type rOCT1 or rOCT1(L447Y,Q448E) with IC_{50} values of 198 and 5.3 μM, respectively (Gorboulev et al., 2005). In the previous experiments, we preincubated the oocytes with corticosterone and measured TEA^+ uptake after 30-min incubation with [^{14}C]TEA^+ in the presence of corticosterone. These experimental conditions do not allow us to distinguish whether the mutations change the affinity of corticosterone to the outward- or inward-facing substrate binding cleft because corticosterone slowly permeates the plasma membrane by passive diffusion (Arndt et al., 2001; Volk et al., 2003). To measure the interaction of corticosterone with the outward-facing cleft, we superfused oocytes for 45 s at −50 mV with 0.2 or 2 mM TEA^+ in the presence of various concentrations of corticosterone and determined the $IC_{50(cort.)}$ values (Table 1). The $IC_{50(cort.)}$ values from current measurements with 2 mM TEA^+ were 3.5 to 4.7 times higher than from measurements with 0.2 mM TEA^+. Because for competitive and noncompetitive inhibition factors of 7.59 and 1 are predicted, respectively, the interaction between TEA^+ and corticosterone can be described as partially competitive. Considering the observed degrees of partial competition (see *Materials and Methods*), we estimated the K_i values for corticosterone [$K_{i(cort.)}$] from the $IC_{50(cort)}$ values from current measurements with 0.2 mM TEA^+ (Figs. 2, 3, and 5; Table 1).

For inhibition of wild-type rOCT1 and rOCT1(C451M) by extracellular corticosterone, respective $K_{i(cort.)}$ values of 27.8 ± 7.2 and 18.4 ± 1.9 μM were estimated (Fig. 2, Table 1). Because these values are not significantly different, the data suggest that the exchange of Cys451 by methionine does not alter the affinity of corticosterone to the outward-facing substrate-binding pocket. Significantly lower $IC_{50(cort.)}$ and $K_{i(cort.)}$ (3.3 ± 0.3 μM) values were obtained for corticosterone inhibition of TEA^+ currents in rOCT1(C451M,L447Y,Q448E) versus the control rOCT1(C451M) (Figs. 2 and 3; Table 1). To elucidate whether the mutation L447Y or Q448E is responsible for the affinity increase, we measured the inhibition of TEA^+-induced currents by corticosterone in the mutants rOCT1(C451M,L447Y) and rOCT1(C451M,Q448E) (Fig. 3; Table 1). For rOCT1(C451M,L447Y) a $K_{i(cort.)}$ of 5.0 ± 0.5 μM was obtained (Fig. 3; Table 1). This value is significantly lower than the $K_{i(cort.)}$ of rOCT1 or rOCT1(C451M) and similar to the $K_{i(cort.)}$ of rOCT1(C451M,L447Y,Q448E). The data indicate that the L447Y mutation is responsible for the increase in affinity for corticosterone from the extracellular side. The $K_{i(cort.)}$ value estimated for mutant rOCT1(C451M,Q448E) (20.0 ± 4.2 μM) is consistently not significantly different from wild-type rOCT1 or rOCT1(C451M) (Fig. 3, Table 1).

Inhibition of rOCT1 and Mutants by Intracellular Corticosterone. To measure the affinity of corticosterone to the

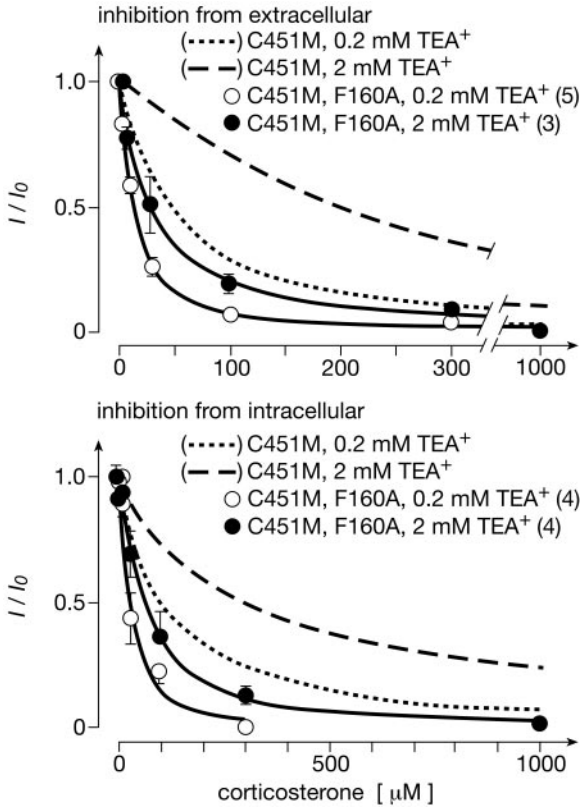

Fig. 5. Effects of the replacement of Phe160 in rOCT1(C451M) by alanine on inhibition of TEA^+-induced currents by extracellular and intracellular corticosterone. Oocytes expressing rOCT1(C451M,F160A) were clamped to −50 mV, and inhibition of TEA^+-induced currents by extracellular or intracellular corticosterone was measured. For inhibition from extracellular, oocytes were superfused with 45-s pulses of Ori buffer containing 0.2 or 2 mM TEA^+ plus various concentrations of corticosterone followed by short wash with Ori buffer. For inhibition from intracellular, oocytes were incubated for 10 min with Ori buffer containing corticosterone, washed with Ori buffer, and currents induced by 0.2 or 2 mM TEA^+ were measured. Currents (I) were normalized to currents in the absence of corticosterone (I_0). Mean values + S.E.M with numbers of analyzed oocytes in parentheses are shown. The curves were obtained by fitting the Hill equation to compiled data sets. The data show that the affinity of extracellular and intracellular corticosterone to rOCT1 was increased upon replacing Phe160 by alanine..

inward-facing substrate binding cleft, oocytes expressing mutants of rOCT1 were preincubated for 10 min with various concentrations of corticosterone, extracellular corticosterone was then removed by washing, and inward currents induced by superfusion with 0.2 or 2 mM TEA^+ were measured. In oocytes expressing rOCT1(C451M) or rOCT1(C451M,Q448E), the IC_{50} values for corticosterone inhibition of currents induced by 2 mM TEA^+ are 2.6 or 2 times higher, respectively, compared with those induced by 0.2 mM TEA^+ (Fig. 4; Table 1). This suggests some competition between intracellular corticosterone and TEA^+ that had entered the oocytes during the measurements. By contrast, in oocytes expressing rOCT1(C451M,L447Y), similar $IC_{50(cort.)}$ values were obtained for inhibition of currents induced by 0.2 mM or 2 mM TEA^+ (Fig. 4, Table 1). This indicates that TEA^+ does not replace corticosterone from the inward-facing cleft of this mutant.

In oocytes expressing rOCT1(C451M), intracellular corticosterone inhibited inward currents by 0.2 mM TEA^+ with an $IC_{50(cort.)}$ value of 132 ± 34 μM (Fig. 4, Table 1). Considering the small degree of competition between intracellular corticosterone and TEA^+, a $K_{i(cort.)}$ value of 71 ± 19 μM was obtained (Table 1). This value is significantly higher compared with the $K_{i(cort.)}$ for corticosterone inhibition from the extracellular side ($P < 0.001$), suggesting that intracellular corticosterone binds with lower affinity to rOCT1 than corticosterone present at the extracellular side. This is at variance with rOCT2, where corticosterone binds with higher affinity from the intracellular side (Volk et al., 2003).

In oocytes expressing rOCT1(C451M,L447Y), $IC_{50(cort.)}$ values of 28 ± 4 μM (0.2 mM TEA^+) and 25 ± 3 μM (2 mM TEA^+) were determined, and a $K_{i(cort.)}$ value of 28 ± 4 μM was estimated (Fig. 4, Table 1). It is noteworthy that this $K_{i(cort.)}$ value is significantly lower than the $K_{i(cort.)}$ value of rOCT1(C451M) from the intracellular side. The data indicate that replacement of Leu447 by tyrosine increases the affinity

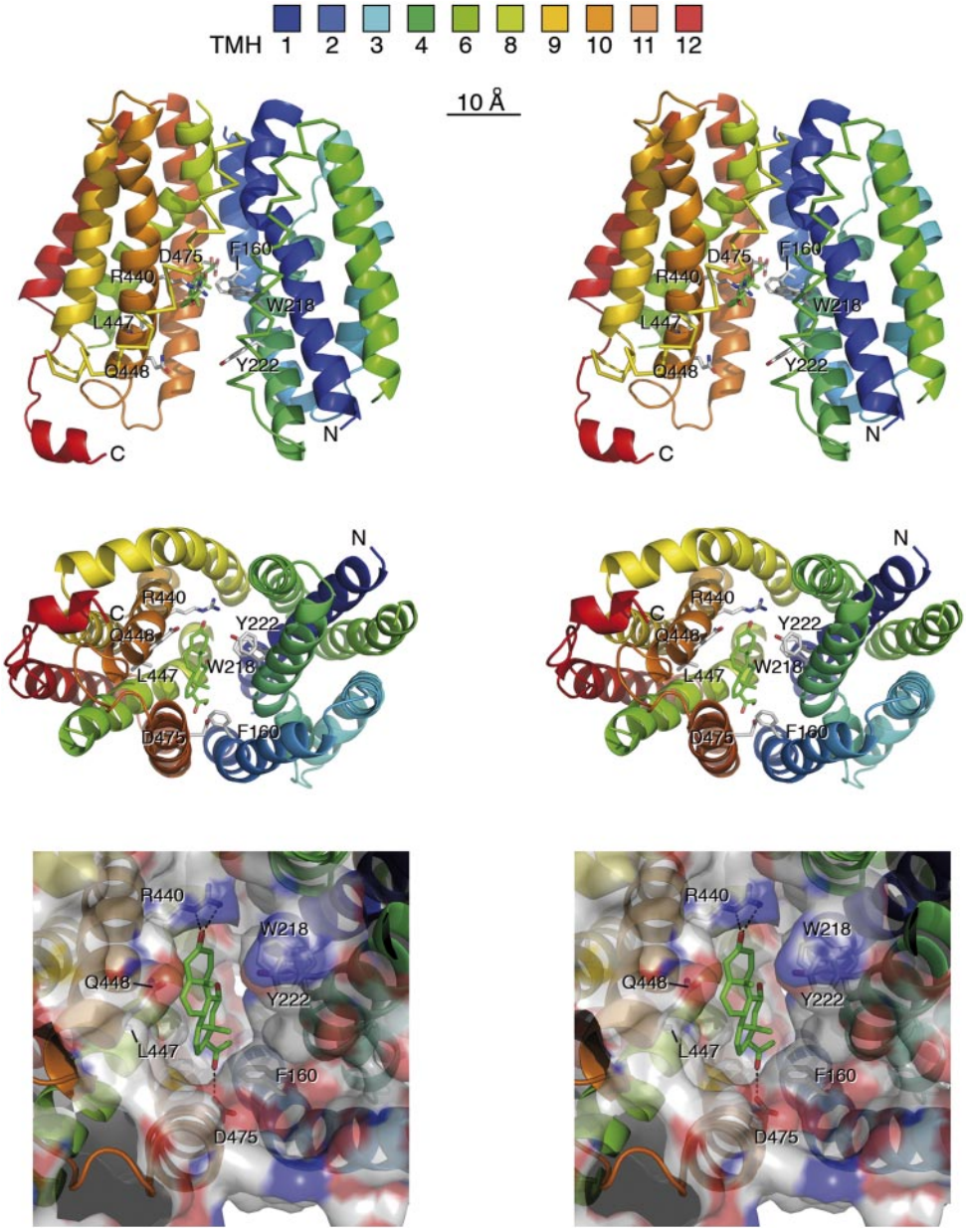

Fig. 6. Docking of corticosterone to the inward-facing substrate cleft of rOCT1. Stereopictures are presented showing a side view with cytosolic N and C termini (top) and views into the binding cleft from the cytosol (middle and bottom). The α-helices in the upper and middle panels are shown as ribbon except for TMH5 (light green) and TMH7 (green), which are presented as Cα-trace in the side view for clarity. The color of the predicted α-helices is indicated. The amino acid side chains of Phe160, Trp218, Tyr222, Arg440, Leu447, Gln448, and Asp475 are shown as sticks. The bottom shows a magnification in which the van der Waals surface of the binding cleft is colored according to amino acid polarity, with hydrophobic residues marked in gray, polar uncharged residues in green, negatively charged residues in red, and positively charged amino acids in blue. Their positions are indicated by numbers. Putative hydrogen bonds between corticosterone (highest docking energy) and amino acids of rOCT1 are indicated by stippled lines.

of corticosterone to both the outward- and inward-facing substrate pockets.

We also measured the effect of replacement of Gln448 by glutamate on the affinity of intracellular corticosterone (Fig. 4). In oocytes expressing rOCT1(C451M,Q448E), intracellular corticosterone inhibited TEA^+-induced inward currents with a $K_{i(cort.)}$ of 2.7 ± 0.4 μM. This is significantly lower than the $K_{i(cort.)}$ determined for intracellular interaction of corticosterone with rOCT1(C451) (Table 1). It is also significantly lower than the $K_{i(cort.)}$ value of 20.0 ± 4.2 μM estimated for the extracellular interaction of corticosterone with rOCT1(C451M,Q448E) ($P < 0.001$). The data indicate that the higher affinity of corticosterone to the inward- compared with the outward-facing substrate-binding pocket of rOCT2 can be transferred to rOCT1 by exchange of Gln448 with glutamic acid located in the corresponding position of rOCT2.

First-Round Simulations of Corticosterone Binding to the Outward- and Inward-Facing Clefts of rOCT1. To distinguish whether the identified amino acids interact directly with corticosterone or exhibit indirect effects on the corticosterone binding site(s), we modeled the interaction of corticosterone with rOCT1. Previously we described a model of the inward-facing conformation of rOCT1, which was obtained from the crystal structure of *E. coli* LacY that belongs to the same superfamily as rOCT1 (Popp et al., 2005). The quality of this model was demonstrated by showing that seven amino acids that are critical for substrate affinity and/or selectivity line the solvent-accessible surface of the modeled inward-open cleft. Using the alternating access transport model of LacY that has been derived on the basis of sophisticated functional and biophysical data (Smirnova et al., 2006; Kaback et al., 2007; Majumdar et al., 2007), we also

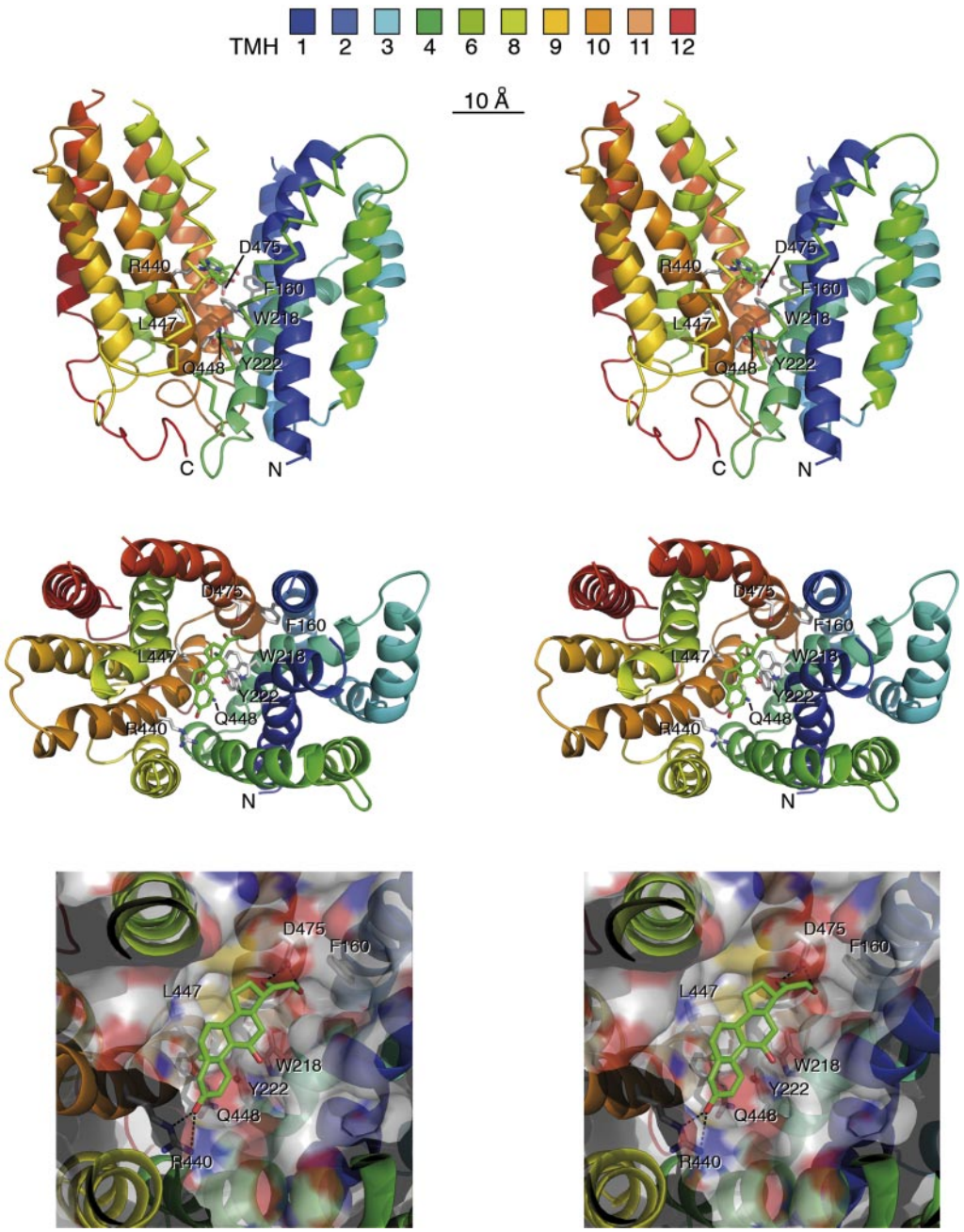

Fig. 7. Docking of corticosterone to the outward-facing substrate cleft of rOCT1. A side view (top) and views from the extracellular side (middle and bottom) are shown. At the top and middle, the α-helices are shown as ribbon except for TMH5 (light green) and TMH7 (green), which are presented as Cα-trace in the side view. The side chains of the numbered amino acids are shown as sticks. The bottom shows a view from the extracellular side in which the van der Waals surface of the binding cleft is coloured according to amino acid polarity (grey, hydrophobic; green, uncharged polar; red, negatively charged; blue, positively charged). At bottom, putative hydrogen bonds with the highest docking energies are indicated by stippled lines.

modeled the outward-facing conformation of rOCT1 (Gorbunov et al., 2008). In the present study, the interactions of corticosterone with the outward- and inward-facing conformation of rOCT1 were simulated by docking of corticosterone to the transporter models. Twenty-eight of 30 corticosterone molecules that docked with the highest scores to the inward-facing cleft of rOCT1, and the 30 corticosterone molecules that docked with the highest scores to the outward-facing cleft, have distances to Leu447 smaller than 10.6 Å (center of gravity used for corticosterone, thus the shortest distance between Leu447 and corticosterone is usually between 5 and 6 Å). We used the results with the smallest distances between corticosterone and Leu447 to select additional amino acid candidates that may be accessible for interaction with extracellular and intracellular corticosterone for mutagenesis experiments. By using this procedure, Phe160 in TMH2 and Tyr222 in TMH4 could be identified as good candidates.

Inhibition of rOCT1(C451M,F160A) and rOCT1-(C451M,Y222F) by Corticosterone. We tested whether the replacement of Phe160 by alanine or of Tyr222 by phenylalanine would change the affinities for extracellular and/or intracellular corticosterone. First we determined whether the affinity of TEA^+ is altered in rOCT1(C451M,F160A). For currents induced by TEA^+ at −50 mV, an $I_{0.5(TEA)}$ value was obtained (98 ± 13 μM, $n = 4$) that is similar to those of rOCT1(C451M) and rOCT1. Extracellular corticosterone inhibited TEA^+-in-

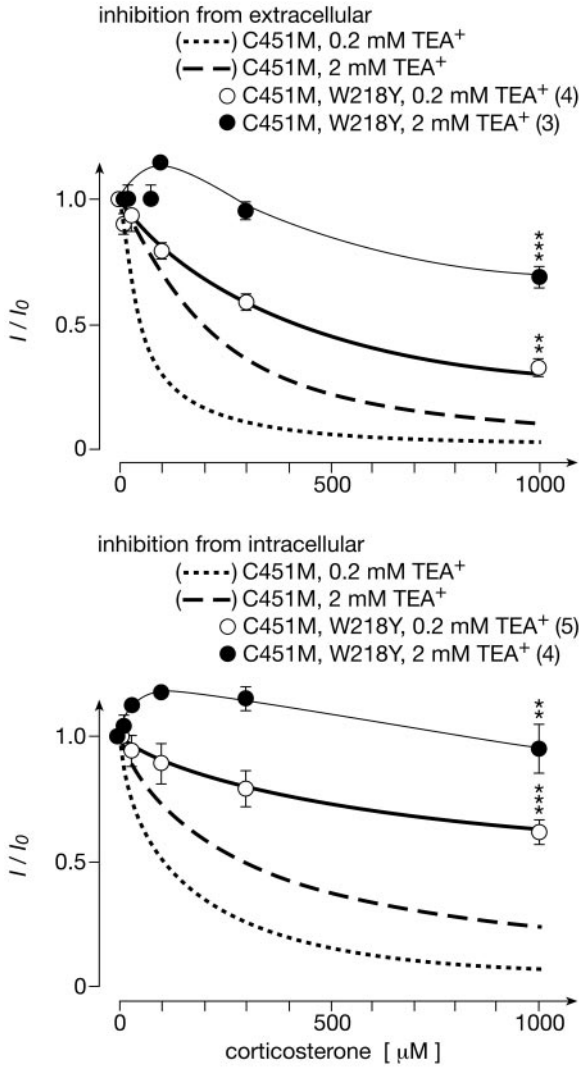

Fig. 8. Effects of replacement of Trp218 by tyrosine on inhibition of TEA^+-induced currents by extracellular and intracellular corticosterone. Oocytes expressing rOCT1(C451M,W218Y) were clamped to −50 mV, and inhibition of TEA^+-induced currents by extracellular or intracellular corticosterone was measured. For inhibition from extracellular, oocytes were superfused with 45-s pulses of Ori buffer containing 0.2 or 2 mM TEA^+ plus various concentrations of corticosterone followed by a short wash with Ori buffer. For inhibition from intracellular, oocytes were incubated for 10 min with Ori buffer containing corticosterone, washed with Ori buffer, and currents induced by superfusion with Ori buffer containing 0.2 or 2 mM TEA^+ were measured. Currents (I) were normalized to currents in the absence of corticosterone (I_0). Mean values ± S.E.M with numbers of analyzed oocytes in parentheses are shown. The curves were obtained by fitting the Hill equation to compiled data sets. The data suggest that the affinity for inhibition by extracellular corticosterone was decreased and indicate that maximal inhibition by intracellular corticosterone was decreased when Trp218 was replaced by tyrosine.

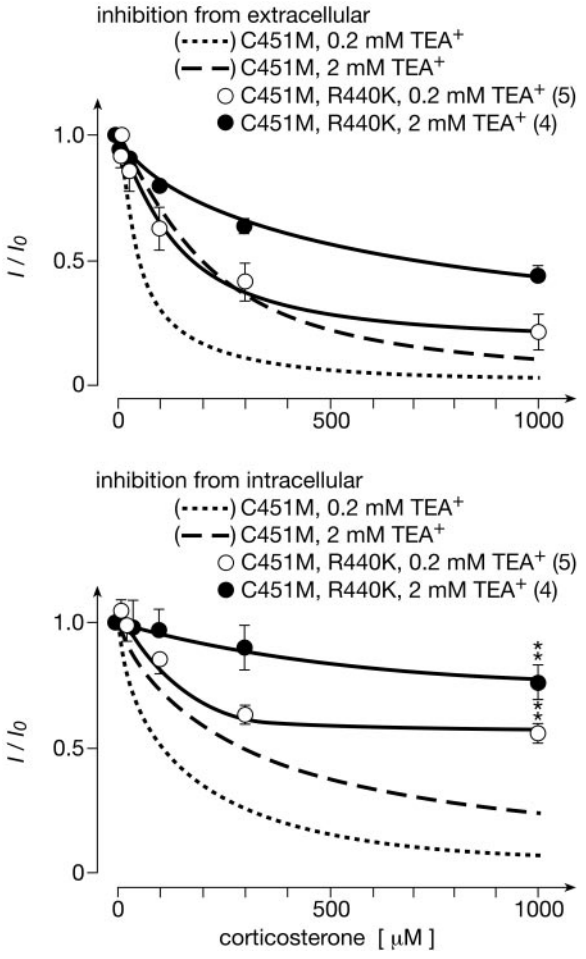

Fig. 9. Effects of replacement of Arg440 by lysine on inhibition of TEA^+-induced currents by extracellular and intracellular corticosterone. Oocytes expressing rOCT1(C451M,R440K) were clamped to −50 mV, and inhibition of TEA^+-induced currents by extracellular or intracellular corticosterone was measured. For inhibition from extracellular, oocytes were superfused with 45-s pulses of Ori buffer containing 0.2 or 2 mM TEA^+ plus various concentrations of corticosterone followed by short wash with Ori buffer. For inhibition from intracellular, oocytes were incubated for 10 min with Ori buffer containing corticosterone, washed with Ori buffer, and currents induced by superfusion with Ori buffer containing 0.2 or 2 mM TEA^+ were measured. Currents (I) were normalized to currents in the absence of corticosterone (I_0). Mean values ± S.E.M with numbers of analyzed oocytes in parentheses are shown. The curves were obtained by fitting the Hill equation to compiled data sets. By this mutation the maximal inhibition by intracellular corticosterone was reduced.

duced currents by rOCT1(C451M,F160A) with a $K_{i(cort.)}$ value of 6.9 ± 1.8 μM, which is significantly smaller compared with rOCT1(C451M) or rOCT1 (Fig. 5, Table 1). It is noteworthy that a significantly smaller $K_{i(cort.)}$ value for rOCT1(C451M,F160A) compared with rOCT1(C451M) was also determined when corticosterone was applied from the intracellular side (18 ± 4 versus 71 ± 19 μM) (Fig. 5; Table 1). Previous data showed that exchange of Tyr222 by phenylalanine decreased the K_m value for [^{14}C]TEA$^+$ uptake (Popp et al., 2005). Consistent with the previous data, the $I_{0.5(TEA)}$ value for currents induced by TEA$^+$ (−50 mV) was decreased in rOCT1(C451M, Y222F) compared with rOCT1(C451M) (39 ± 2 versus 65 ± 18 μM, $n = 5$ each, $P < 0.05$). In oocytes expressing rOCT1(C451M,Y222F), $K_{i(cort.)}$ values of 26.2 ± 1.7 and 69 ± 15 μM were determined for inhibition of TEA$^+$-induced currents by extracellular and intracellular corticosterone, respectively (Table 1). The values are similar to the $K_{i(cort.)}$ values measured in oocytes expressing rOCT1(C451M) or rOCT1 (Table 1). The data suggest that Phe160 participates in binding of extracellular and intracellular corticosterone to rOCT1 and that Tyr222 is not critically involved in corticosterone binding.

Second-Round-Simulations of Corticosterone Binding. Because the above-described mutagenesis experiments revealed that the affinities of corticosterone to both the outward- and the inward-facing conformations of rOCT1 were increased when Leu447 in TMH10 was replaced by tyrosine or when Phe160 in TMH2 was replaced by alanine, we performed a new set of docking simulations in which residues Leu447 and Phe160 were selected as direct docking sites using radii of 5 Å around these residues. The obtained 30 docking sites for corticosterone with the highest interaction energies for the outward- and inward-facing conformation of rOCT1 clustered into families of conformers with similar distances between corticosterone and the target amino acids but slightly different orientations of corticosterone in the putative binding pocket. Figure 6 shows one example for the interaction of corticosterone with the inward-facing cleft. Note that the model is consistent with the interaction of corticosterone with Phe160 (distance, 2.6 Å) and Leu447 (distance, 4.9 Å). It also suggests an interaction with Trp218 in TMH4 (distance, 4.0 Å), Arg440 in TMH10 (distance 2.8 Å), and Asp475 in TMH11 (distance, 2.8 Å). The docking model does not support a direct interaction of corticosterone with Tyr222 (distance, 8.5 Å) and Gln448 (distance, 7.6 Å). We speculate that the affinity increase for intracellular corticosterone observed after exchange of Gln448 by glutamate might be due to an allosteric effect on Leu447.

In Fig. 7, an example for the interaction of corticosterone with the outward-facing substrate binding cleft is shown. The figures show that corticosterone is located close to Phe160 (3.6 Å), Leu447 (5.0 Å), Trp218 (3.0 Å), Arg440 (3.1 Å), and Asp475 (2.8 Å). The distances from corticosterone to Tyr222 (6.0 Å) and Gln448 (6.4 Å) are larger and do not yield a direct van der Waals contact. This is consistent with the missing effects of these mutations on inhibition of rOCT1 by extracellular corticosterone.

Affinity of Corticosterone to rOCT1(C451M,W218Y) and rOCT1(C451M,R440K). The modeled interactions of corticosterone with rOCT1 predict that mutations of Trp218, Arg440, and Asp475 can change the inhibition of TEA$^+$-induced currents by intracellular and extracellular corticosterone. For TEA$^+$-induced currents by rOCT1(C451M, W218Y) and by rOCT1(C451M,R440K) measured at −50 mV, $K_{0.5(TEA)}$ values of 67 ± 4 and 67 ± 6 μM ($n = 3$, each) were determined. Because these values are similar to rOCT1 and rOCT1(C451M), the two amino acids are not critical for the affinity of TEA$^+$ to stimulate inward currents. In Fig. 8, we measured TEA$^+$-induced currents by rOCT1(C451M,W218Y) in the presence of extracellular or intracellular corticosterone. With 1 mM corticosterone applied to the extracellular or intracellular side, a significantly lower inhibition was observed compared with rOCT1(C451M) or wild-type rOCT1 ($P < 0.01$ for difference). This suggests a reduced maximal inhibition and is consistent with an interaction of extracellular and intracellular corticosterone with Trp218. Using the variant rOCT1(C451M,W218Y), we also observed an atypical stimulation at low concentrations of extracellular or intracellular corticosterone on currents that were induced by 2 mM TEA$^+$. This stimulation may be explained by binding of corticosterone to a high-affinity binding site (Volk et al., 2003), which may be located in a peripheral part of the binding cleft and may stimulate TEA-induced current in this specific mutant. The low degree of maximal inhibition and the atypical curves obtained with 2 mM TEA$^+$ prevents a determination of $IC_{50(cort.)}$ values for most experimental conditions. For partial inhibition of 0.2 mM TEA$^+$-induced currents by extracellular corticosterone, we determined an $IC_{50(cort)}$ value of 333 ± 42 μM ($n = 4$). Assuming competitive inhibition we estimated a minimal $K_{i(cort.)}$ value (93.3 ± 11.8 μM), which is significantly higher than the $K_{i(cort.)}$ values obtained for rOCT1 or rOCT1(C451M; Table 1).

Figure 9 shows corticosterone inhibition of TEA$^+$-induced currents in oocytes expressing rOCT1(C451M,R440K). For inhibition of TEA$^+$-induced currents with extracellular corticosterone IC_{50} values of 112 ± 15 μM (0.2 mM TEA$^+$) and 588 ± 124 μM (2 mM TEA$^+$) were determined suggesting partial competitive inhibition (Table 1). The estimated K_i value of 40.4 ± 5.3 μM is significantly higher compared with rOCT1 wild-type or rOCT1(C451M). The maximal inhibition of rOCT1(C451M,R440K) by intracellular corticosterone is significantly smaller compared with rOCT1(C451M) or wild-type rOCT1. Upon preincubation of oocytes expressing

TABLE 2

Effect of mutations that change the interaction of corticosterone with rOCT1 on the affinity of MPP$^+$

Inhibition of [^{14}C]TEA$^+$ uptake by MPP$^+$ was measured in oocytes expressing wild-type rOCT1 or rOCT1 mutants. Oocytes were incubated 15 min with 5 μM [^{14}C]TEA$^+$ in the presence of eight different concentrations of MPP$^+$. $IC_{50(MPP)}$ values of individual experiments were determined by fitting the Michaelis-Menten equation to the data. Mean values ± S.E.M. are presented. Numbers of independent experiments are indicated in parenthesis.

Mutation	$IC_{50(MPP)}$
Wild type	7.4 ± 1.1 (3)
C451M	9.4 ± 1.3 (4)
C451M, L447Y	0.46 ± 0.09** (3)
C451M, Q448E	2.5 ± 0.52* (3)
C451M, L447Y, Q448E	0.31 ± 0.05** (3)
C451M, F160A	19.5 ± 2.0** (3)
C451M, W218Y	23.1 ± 2.2*** (3)
C451M, R440K	18.6 ± 2.2** (3)

* $P < 0.05$, significance for difference compared to rOCT1(C451M) mutant calculated by ANOVA with post hoc Tukey test.

** $P < 0.01$, significance for difference compared to rOCT1(C451M) mutant calculated by ANOVA with post hoc Tukey test.

*** $P < 0.001$, significance for difference compared to rOCT1(C451M) mutant calculated by ANOVA with post hoc Tukey test.

rOCT1(C451M,R440K) with 1 mM corticosterone, currents induced by 0.2 mM TEA^+ were inhibited by 44 ± 4 versus 93 ± 5% in oocytes expressing rOCT1(C451M) ($P < 0.01$ for difference). For inhibition by intracellular corticosterone of currents induced by 0.2 mM TEA, an IC_{50} value of 124 ± 33 μM could be obtained (Table 1). This value is similar to the IC_{50} value of wild-type rOCT1, suggesting an unaltered affinity for corticosterone. The data showing reduced affinity of extracellular corticosterone and reduced maximal inhibition by intracellular corticosterone are consistent with an interaction of corticosterone with Arg440 in the outward- and inward-facing conformations.

Because mutations of Asp475 block or drastically reduce organic cation transport by rOCT1 in oocytes (Gorboulev et al., 1999), effects of mutations in this position on the inhibition of TEA^+-induced currents by extracellular versus intracellular corticosterone could not be investigated. However, in HEK293 cells stably transfected with rOCT1(D475E), the inhibition of [^{3}H]MPP uptake by extracellular or intracellular corticosterone could be measured. Uptake measurements were performed using a 1-s incubation period with 0.013 μM [^{3}H]MPP^+. Inhibition by extracellular corticosterone was measured by performing 1-s incubation with [^{3}H]MPP^+ in the presence of corticosterone. To measure inhibition by intracellular corticosterone, the cells were preincubated for 10 min with corticosterone. Thereafter, the cells were diluted with 15-fold excess of corticosterone-free buffer containing 0.013 μM [^{3}H]MPP^+, and uptake of MPP^+ was measured after 1-s incubation. For inhibition of wild-type rOCT1 and rOCT1(D475E) mutant by extracellular corticosterone, $K_{i(cort)}$ values of 6.9 ± 0.9 and 72.5 ± 11.8 μM were determined, respectively ($P < 0.001$ for difference, $n = 3$ each). The $K_{i(cort)}$ values for inhibition by intracellular corticosterone were 8.5 ± 1.0 μM for rOCT1 versus 357 ± 55 μM for rOCT1(D475E) ($P < 0.01$ for difference, $n = 3$ each).[1]

Effects of Mutations Changing the Interaction of Corticosterone on the Affinity of MPP^+. We determined the $IC_{50(MPP)}$ values for inhibition of [^{14}C]TEA^+ (5 μM) uptake by MPP^+ (Table 2). Because 5 μM [^{14}C]TEA^+ used for uptake was more than 10-fold smaller than the K_m values for TEA^+ in wild-type rOCT1 and the tested mutants, the obtained $IC_{50(MPP)}$ values are basically identical to the $K_{i(MPP)}$ values. Confirming previous data (Arndt et al., 2001; Gorboulev et al., 2005), we obtained similar $IC_{50(MPP)}$ values for rOCT1 (7.4 ± 1.1 μM) and rOCT1(C451M) (9.4 ± 1.3 μM). We observed previously that in the mutant rOCT1(L447Y, Q448E), the K_i value for inhibition of [^{14}C]TEA^+ uptake by MPP^+ ($K_{i(MPP)}$) was decreased 10-fold compared with rOCT1 (Gorboulev et al., 2005). The $IC_{50(MPP)}$ value of rOCT1-(C451M,L447Y,Q448E) was approximately 20-fold lower (0.31 ± 0.05 μM). A similar low $IC_{50(MPP)}$ value was obtained for rOCT1(C451M,L447Y) (0.46 ± 0.09 μM). It is noteworthy that the $IC_{50(MPP)}$ value of rOCT1(C451M,Q448E) (2.5 ± 0.52 μM) was significantly smaller than those of rOCT1 or rOCT1(C451M). Both mutations, L447Y and Q448E, apparently increase the affinity of MPP^+; however, their effects are not additive.

For mutants F160A, W218Y, and R440K, a decreased affinity of MPP^+ to inhibit [^{14}C]TEA^+ uptake was observed (Table 2). $IC_{50(MPP)}$ values of 19.5 ± 2.0 μM [rOCT1(C451M, F160A)], 23.1 ± 2.2 μM [rOCT1(C451M,W218Y)] and 18.6 ± 2.2 μM [rOCT1(C451M,R440K)] were determined. Previous data showed that the affinity of MPP^+ was not changed when Asp475 was replaced by glutamate (Gorboulev et al., 1999). The data suggest that Phe160, Trp218, Arg440, Leu447, and Gln448 are located within or close to the transport-relevant binding site for MPP^+ and that this MPP^+ binding site is located within the innermost cavity of the binding cleft where corticosterone also binds.

Effects of Mutations Changing the Interaction of Corticosterone on the Affinity of $TBuA^+$. We investigated whether mutations L447Y, F160A, W218Y, and R440K altered the inhibition of TEA^+-induced currents (−50 mV) by the nontransported rOCT1 inhibitor $TBuA^+$ (Table 3; Fig. 10). In the mutants rOCT1(C451M,F160A) and rOCT1-(C451M,L447Y), the affinity for $TBuA^+$ was increased at least 10-fold compared with rOCT1(C451M), whereas it was unaltered in rOCT1(C451M,W218Y) and rOCT1(C451M, R440K). The increase of the $IC_{50(TBuA)}$ values for inhibition of currents induced by 2 mM TEA^+ versus 0.2 mM TEA^+ suggest competitive inhibition for the mutants rOCT1(C451M), rOCT1(C451M,L44Y), rOCT1(C451M,W218Y), and rOCT1-(C451M,R440K). In case of rOCT1(C451M,F160A), we observed a significantly higher difference of $IC_{50(TBuA)}$ values obtained with 2 mM TEA^+ versus 0.2 mM TEA^+ (15.8-fold), as expected for competitive inhibition (7.6-fold). This suggests allosteric effects of TEA^+ binding on $TBuA^+$ binding. Previous data showed that the affinity of $TBuA^+$ to inhibit uptake of TEA^+ was increased when Asp475 was replaced by glutamate (Gourboulev et al., 1999). The data suggest that Phe160, Leu447, and Asp475 are involved in binding of extracellular $TBuA^+$ in addition to extracellular corticosterone.

[1] Note that the $K_{i(cort.)}$ value for inhibition of wild-type rOCT1 by extracellular corticosterone measured in HEK293 cells was lower compared with the $K_{i(cort.)}$ value measured in *X. laevis* oocytes (Table 1). Recent data suggest that these differences as well as different affinities of some organic cations observed after expression of rOCT1 in HEK293 cells versus oocytes, are due to different regulatory states of rOCT1 in the two expression systems (H. Koepsell, V. Gorboulev, and U. Roth, unpublished data).

TABLE 3

Effects of mutations that change the interaction of corticosterone with rOCT1 on the affinity of $TBuA^+$ from extracellular

Wild-type rOCT1 or rOCT1 mutants were expressed in oocytes. Inhibition of currents induced by superfusion with 0.2 mM or 2 mM TEA^+ by extracellular $TBuA^+$ was measured as in Fig. 2. The Hill equation was fitted to inhibition curves of individual oocytes and IC_{50} values were calculated. The data are presented and the K_i values were calculated as in Table 1. The ratios between the mean IC_{50} values measured with 2 mM TEA^+ and 0.2 mM TEA^+ [$f_{(part.compet.)}$] were used to calculate the K_i values from the IC_{50} value obtained with 0.2 mM TEA^+.

Inhibition from Extracellular	C451M	C451M,F160A	C451M,L447Y	C451M,W218Y	C451M,R440K
IC_{50} (0.2 mM TEA)	11.8 ± 3.6 (6)	1.2 ± 0.2 (5)***	1.1 ± 0.3 (5)***	11.0 ± 0.1 (3)	9.7 ± 2.1 (6)
IC_{50} (2 mM TEA)	81.5 ± 10.5 (4)	19.3 ± 1.7 (6)***	6.4 ± 1.7 (5)***	88.3 ± 14.4 (4)	82.9 ± 16.2 (4)
$f_{(part.compet.)}$	6.9	15.8†	5.8	8.0	8.5
K_i	3.5 ± 1.1	0.18 ± 0.03***	0.30 ± 0.08***	2.89 ± 0.03	2.43 ± 0.53

*** $P < 0.001$, analysis of variance with Tukey test, difference compared with rOCT1(C451M).
† $P < 0.01$, Student's t test, difference from rOCT1(C451M).

Simulation of $TBuA^+$ Binding to the Outward-Facing Cleft of rOCT1. We also simulated the binding of $TBuA^+$ to the outward-facing cleft of our rOCT1 homology model. Several putative interaction sites showed up if all residues lining the interior of the outward-facing cleft were allowed for docking. This may reflect the presence of low- and high-affinity binding sites for $TBuA^+$ that were demonstrated by measuring $TBuA^+$ effects on the fluorescence of rOCT1 labeled with a fluorescent dye (Gorbunov et al., 2008). Because previous data suggested that $TBuA^+$ binds to Asp475 and that Asp475 is located within a transport relevant binding site for TEA^+ (Gorboulev et al., 1999), we performed a simulation in which the allowed distance between $TBuA^+$ and Asp475 was restricted to 6.5 Å (Fig. 11). Simulation of $TBuA^+$ binding under this constraint suggested that $TBuA^+$ binds simultaneously to Asp475 (3.5 Å), Trp218 (4.3 Å), and Phe160 (3.9 Å) but does not interact with Leu447 (7.2 Å), Tyr222 (7.6 Å), and Arg440 (10.9 Å). The observation that the affinity of TBuA was not changed in the W218Y mutant may be due to a similar hydrophobic interaction of $TBuA^+$ with the indole ring of Trp218 and the phenol ring of Tyr218 (Fig. 11, bottom). The distance of 7.2 Å between $TBuA^+$ and Leu447 suggests no interaction in wild-type rOCT1. However, after replacement of Leu447 by tyrosine, the distance to the docked $TbuA^+$ is shortened by approximately 3 Å. This would allow direct contact of $TBuA^+$ with tyrosine in position 447 and may explain why the affinity of $TBuA^+$ was increased in the L447Y mutant (Table 3).

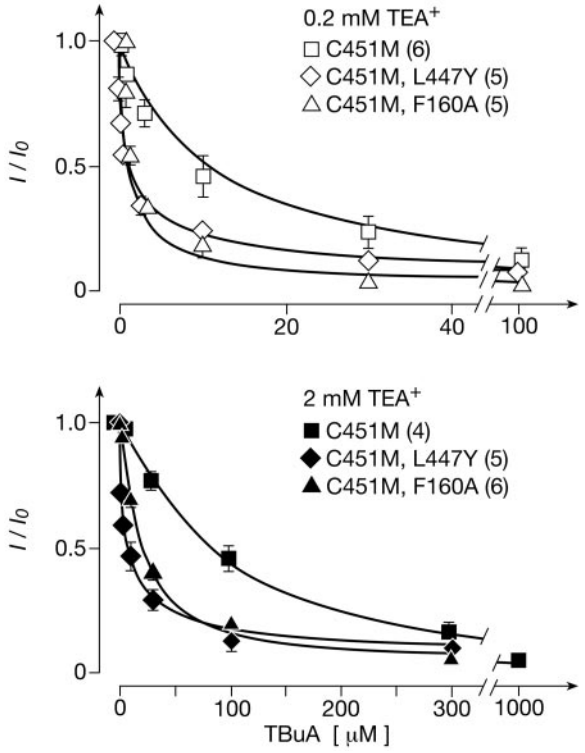

Fig. 10. Effects of replacements of Leu447 by tyrosine and of Phe160 by alanine on inhibition of TEA^+-induced currents by extracellular $TBuA^+$. Mutants rOCT1(C451M), rOCT1(C451M,L447Y), and rOCT1(C451M, F160A) were expressed in oocytes. The oocytes were clamped to −50 mV and superfused with 45-s pulses of Ori buffer containing 0.2 mM TEA^+ plus various concentrations of $TBuA^+$ or 2 mM TEA^+ plus $TBuA^+$. Each pulse with TEA^+ was followed by short wash with Ori buffer. Currents (I) were normalized to currents measured in the absence of $TBuA^+$ (I_0). Mean values + S.E.M with numbers of analyzed oocytes in parentheses are shown. The curves were obtained by fitting the Hill equation to compiled data sets. The affinity for extracellular $TBuA^+$ was increased by exchange of Leu447 by tyrosine and of Phe160 by alanine.

Discussion

We have identified five amino acid residues located within the central part of the transport path of rOCT1 that are critical for the inhibition of rOCT1 by extracellular and intracellular available corticosterone. These amino acids contribute to the modeled outward- and inward-facing binding sites for corticosterone and are located within innermost cavities of the binding clefts. Our data suggest that three of these amino acids are also critical for binding of the nontransported inhibitor $TBuA^+$ from the extracellular side. Four of the amino acids within the innermost cavities are likely to also be involved in binding of the substrate MPP^+, whereas one amino acid probably interacts with TEA^+.

Analysis of Corticosterone Interaction with rOCT1. To determine the interaction of corticosterone from both sides of the plasma membrane, electrical measurements in voltage-clamped oocytes expressing rOCT1 mutants were employed. Voltage-clamped conditions were used because corticosterone binding to rOCT2 was shown to be influenced by the membrane potential (Volk et al., 2003). We performed the present study with rOCT1 because several amino acids within the substrate binding region have been identified in this subtype (Gorboulev et al., 1999, 2005; Popp et al., 2005; Gorbunov et al., 2008). A technical problem (i.e., that substrate-induced currents by rOCT1 are 5- to 10-fold lower than those by rOCT2) was solved by introducing the mutation C451M, which increases rOCT1-mediated currents without altering the interaction with corticosterone. To investigate the interaction of extracellular corticosterone with rOCT1, oocytes were superfused for 45 s with TEA^+ in the presence of corticosterone. During this period, passive permeation of corticosterone across the plasma membrane can be neglected because the inhibitory effect of corticosterone could be reversed by a short wash. To investigate the interaction of corticosterone from the intracellular side, we preincubated the oocytes for 10 min with corticosterone, removed the extracellular corticosterone by washing, and measured currents that were induced by a short superfusion with TEA^+. The intracellular concentration of corticosterone was estimated by assuming that corticosterone had fully equilibrated within the intracellular aqueous phase. The validity of this assumption was verified by control experiments with rOCT1 (see *Materials and Methods*) and in previous experiments with rOCT2 in which preincubation with intact oocytes was compared with measurements using inside-out giant patches (Volk et al., 2003).

Because corticosterone was supposed to interact with the substrate binding region of rOCT1 that includes a binding site for TEA^+, we measured TEA^+- induced currents at two different TEA^+ concentrations. This allowed us to determine the degree of competition between corticosterone and TEA^+ and to estimate the apparent K_i value for corticosterone. Effects of mutations on the K_i value for inhibition of TEA^+ induced currents are supposed to reflect changes at the binding site for corticosterone. The degree of competition between TEA^+ and corticosterone may be changed when the corticosterone binding site, the TEA^+ binding site, or an overlap-

ping part of both binding sites is altered. Another possibility is that a short-term allosteric interaction between the two sites is affected. In wild-type rOCT1 and the rOCT1(C451M) mutant we observed competition between TEA^+ and extracellular as well as intracellular corticosterone. This competition was affected by some of the applied mutations. At the outward-facing corticosterone binding site, the degree of competition between corticosterone and TEA^+ was unaltered when Leu447 was replaced by tyrosine but was decreased when Phe160 was exchanged for alanine. By contrast, intracellular competition between corticosterone and TEA^+ was abolished when Leu447 was replaced by tyrosine, whereas it was not changed in the F160A mutant [Table 1, compare $f_{(\text{part.compet.})}$ values]. These effects suggest different orientations and/or positions of Phe160 and Leu447 in the outward- versus the inward-facing conformation.

TEA^+ probably does not bind directly to the four amino acids that interact with corticosterone (Phe160, Trp218, Arg440, Leu447) because the $I_{(0.5)}$ values for TEA^+-induced currents were not altered by mutations in these positions. However, the TEA^+ binding site supposedly overlaps with the binding site of corticosterone, because Asp475, which is critical for the affinity of TEA^+ (Gorboulev et al., 1999), is located within the modeled innermost cavities and mutation of this site alters the affinity of extracellular and intracellular corticosterone.

Model Analysis of Corticosterone and $TBuA^+$ Binding. Modeling of the inward-open and outward-open conformations of rOCT1 on the basis of LacY permease has been discussed in detail earlier (Popp et al., 2005; Gorbunov et al., 2008). The sequence identity between rOCT1 and LacY is low (~12%); however, different sequence alignment programs produced consistent alignments. LacY-based models of rOCT1 exhibited no steric clashes after refinement, indicating a similar packing in OCT1 and LacY. The quality of the modeled inward-facing conformation is exemplified by the observation that seven amino acids that are critical for affinities of substrates line the inward open cleft (Popp et al., 2005).

The model of the outward-facing conformation of rOCT1 was constructed in analogy to an experimentally verified model of LacY assuming a rigid-body movement of TMHs 1 to 6 with respect to TMHs 7 to 12 allowing intrahelix motions and drifting of individual domains (Gorbunov et al., 2008). An experimental indication for the quality of this model was the observation that amino acids in TMH2 and TMH11 that have contact in the modeled inward-facing conformation and are far apart in the modeled outward-facing conformation proved to be critical for transporter function after high-affinity binding of $TBuA^+$ (Gorbunov et al., 2008).

Being aware of the limitations in modeling ligand-transporter interactions using modeled tertiary structures, our first attempt only aimed to evaluate whether the experimental observation that Leu447 interacts with extracellular and intracellular corticosterone is consistent with the structural models. This turned out to be the case; however, the exact position of corticosterone close to Leu447 was not defined. After Phe160 was identified by mutagenesis as another amino acid that interacts with extracellular and intracellular corticosterone, we performed a second round of docking analyses restricting the distances between corticosterone and the rOCT1 residues Leu447 and Phe160 for distinguishing successful and unsuccessful docking. Using this approach, Trp218, Arg440, and Asp475 were predicted as additional

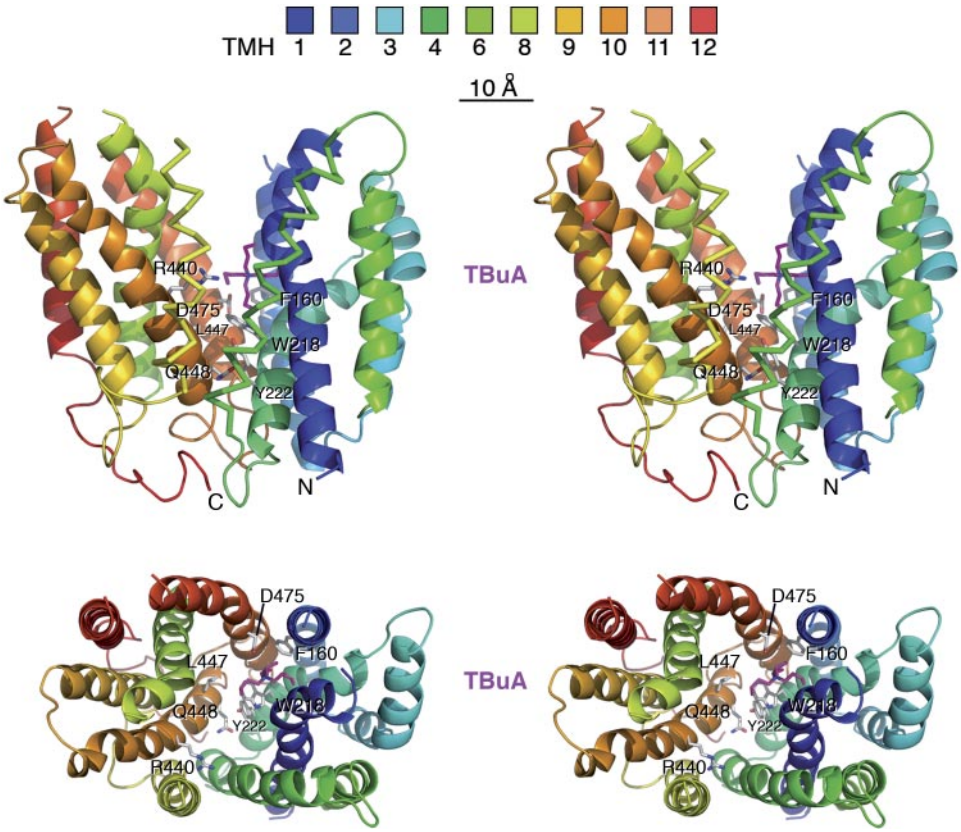

Fig. 11. Docking of $TBuA^+$ to the outward-facing substrate cleft of rOCT1. A side view (top) and a view from the extracellular side (bottom) are shown. The α-helices are shown as ribbon except for TMH5 (light green) and TMH7 (green) at the top, which are presented as Cα-trace. The side chains of the numbered amino acids are shown as sticks.

amino acids interacting with extracellular and intracellular corticosterone. The functional analyses of mutations in these positions are consistent with these predictions. They revealed that the affinity of extracellular corticosterone was decreased after mutation of Trp218, the maximal inhibition by extracellular corticosterone was decreased after mutation of Arg440, and the maximal inhibition by intracellular corticosterone was decreased after mutation of both positions. Note that a mutation of an amino acid interacting with corticosterone must not necessarily change the dissociation constant for corticosterone. It may alter the positioning of bound corticosterone without changing its dissociation constant. This might then lead to an altered degree of maximal inhibition. The modeled position of Asp475 in the outward- and inward-facing binding site of corticosterone was confirmed experimentally by showing that the affinity of extracellular and intracellular corticosterone was decreased when Asp475 was replaced by glutamate. Because most mutations in position 475 block transport activity and the most conservative replacement (D475E) decreases transport activity drastically, a different expression system and a different transport assay had to be employed to determine the affinity of extracellular and intracellular corticosterone to this mutant (H. Koepsell, V. Gorboulev, U. Roth, unpublished data).

The structural models of rOCT1 are also consistent with our observations that the affinity for extracellular corticosterone was unchanged after mutation of Gln448 and that the affinity for corticosterone from both sides was unaltered when Tyr222 was mutated. On first sight, the affinity increase of intracellular corticosterone after mutation of Gln448 seems to contradict our corticosterone-interaction modeling. However, the replacement of Gln448 by glutamate may change the position of Leu447, which directly interacts with corticosterone.

The quality of the modeled outward-facing cleft of rOCT1 was also supported by simulation of $TBuA^+$ binding to the outward-facing cleft and mutagenesis. The simulation revealed several putative $TBuA^+$ interaction sites within the cleft that may represent high- and low-affinity $TBuA^+$ binding sites. We have identified high- and low-affinity interaction of $TBuA^+$ with rOCT1 using voltage-clamp fluorometry (Gorbunov et al., 2008). Mutagenesis at all simulated interaction sites combined with $TBuA^+$ binding measurements is required to identify binding sites with different affinities. Because we hypothesized that the transport relevant $TBuA^+$ binding site is located within the innermost part of the cleft, and previous mutagenesis suggested interaction of Asp475 with $TBuA^+$, we performed a simulation in which the distance of $TBuA^+$ to Asp475 was restricted. This simulation suggests that $TBuA^+$ binds to Phe160 and Trp218 in addition to Asp475. Interaction of $TBuA^+$ with Phe160 is supported by the observed increase of $TBuA^+$ affinity after replacement of Phe160 with alanine (Table 3). So far, the simulated interaction of $TBuA^+$ with Trp218 has not been verified because the affinity of $TBuA^+$ remained unchanged when Trp218 was replaced by tyrosine. This does not contradict our simulation, which predicts a hydrophobic interaction of a butyl side chain of $TBuA^+$ with the aromatic ring system of Trp218, because this interaction may be mimicked by the aromatic ring of tyrosine (Fig. 11, bottom). Future experiments will show whether the affinity of $TBuA^+$ is changed when amino acids with aliphatic side chains are used for substitution of Trp218. Our simulation showing a distance of 6.2 Å between Leu447 and TBuA does not support a direct interaction of $TBuA^+$ with Leu447 in wild-type rOCT1. However, in the L447Y mutant the distance between $TBuA^+$ and Tyr447 should be approximately 3 Å, allowing a direct interaction of $TBuA^+$, which may lead to the observed increase in affinity.

Subtype and Species Differences of Corticosterone Binding. Employing preincubation of oocytes with corticosterone, the rank order of the apparent K_i values for corticosterone inhibition of organic cation uptake is hOCT3 ≪ rOCT3 = rOCT2 ≪ rOCT1 (Gorboulev et al., 2005; Koepsell et al., 2007). Four of the five amino acids that are supposed to be directly involved in corticosterone binding to rOCT1 (Phe160, Trp218, Arg440, and Asp475, numbering of rOCT1) are conserved among rOCT1, rOCT2, rOCT3, and hOCT3, whereas the amino acids in positions 447 differ between rOCT1 versus rOCT2, rOCT3, or hOCT3 (Fig. 12). Because the affinity of corticosterone is similar when tyrosine (rOCT2) or phenylalanine (rOCT3, hOCT3) is placed into position 447 of rOCT1 (C. Volk, V. Gorboulev, H. Koepsell, unpublished data) and rOCT3 and hOCT3 have identical amino acids in all five positions but different affinities to corticosterone, the higher affinities of corticosterone to rOCT2, rOCT3, and hOCT3 versus rOCT1 cannot be exclu-

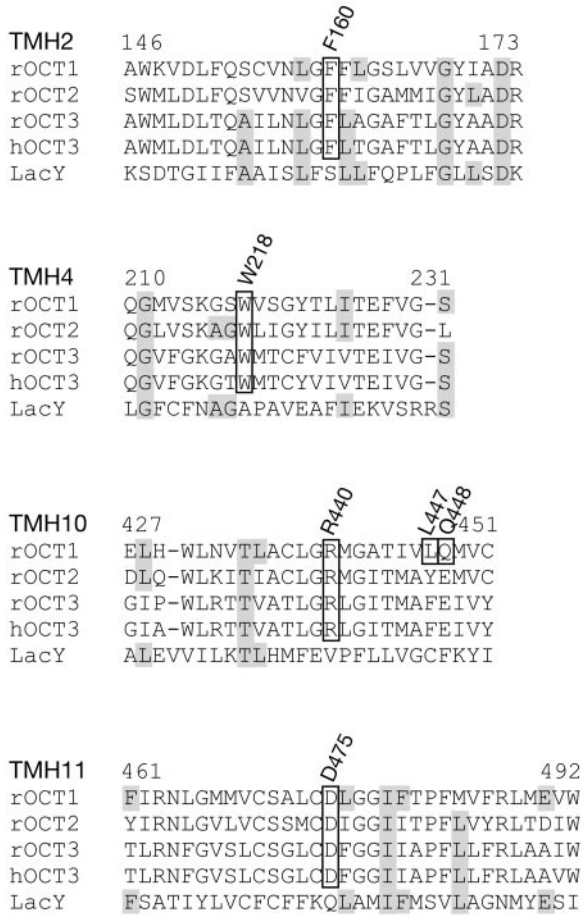

Fig. 12. Sequence alignment of transmembrane helices of OCTs that interact with corticosterone and the corresponding helices of LacY. Amino acids that are conserved between LacY and OCTs are on gray background. Amino acids that are critical for corticosterone interaction with OCT1 are boxed. The amino acids that are conserved between LacY and OCTs are apparently not involved in corticosterone binding.

sively due to differences in position 447. Considering the differences in substrate selectivity between OCT subtypes and OCT3 orthologs, and the overlap between the substrate and corticosterone binding sites, we speculate that the corticosterone binding sites of OCT subtypes and orthologs contain more structural differences than implied from our studies, which have been performed mostly within the rOCT1 backbone. It is possible that not all amino acids that interact with corticosterone in rOCT1 also participate in corticosterone binding to the other subtypes and orthologs.

Mechanism for Transport by rOCT1. Our data, which indicate that outward- and inward-facing innermost cavities in rOCT1 contain several identical amino acids critical for affinities of nontransported inhibitors (corticosterone, $TBuA^+$) and substrates (MPP^+, TEA^+), strongly suggest that rOCT1 operates by an alternating access transport mechanism. In a trans-zero transport cycle, an organic cation binds to the outward-facing innermost cavity, the cavity closes on the extracellular and opens on the intracellular side, the cation is released to the cytosol, and the empty cavity switches back to the outward-facing conformation. Nontransported inhibitors, such as the bulky rectangular corticosterone molecule with the dimensions of $14 \times 7 \times 5$ Å may bind to the innermost cavities and may thereby block the conformational switch. Recently we provided evidence for the existence of high-affinity organic cation binding sites in OCTs and demonstrated that high-affinity binding of organic cations may lead to inhibition of transport (Gorbunov et al., 2008; Minuesa et al., 2009). We speculate that these high-affinity binding sites are located outside the innermost cavities in more peripheral regions of the binding clefts and are not directly involved in translocation.

Recent experimental data also suggest the existence of outward-open and inward-open innermost cavities in rOCT2 and provide support for an alternating access transport mechanism by this subtype (Schmitt et al., 2009). In that study, we observed that small cations are taken up by OCT2 (at 0 mV) together with organic cation substrates and provided evidence that this effect cannot be explained by opening of passive permeabilities during transport. It is noteworthy that the surplus of charge translocation was abolished when Glu448 in the innermost cavity of rOCT2 corresponding to Gln448 in rOCT1 was replaced by glutamine. We speculate that Glu448 and Asp475 within the outward-facing innermost cavity of rOCT2 attract small cations and release them from the inward-facing innermost cavity in which Glu448 is located more peripherally compared with the outward-facing innermost cavity (Figs. 6 and 7).

Acknowledgments

We thank Michael Christof for preparing the figures.

References

Abramson J, Smirnova I, Kasho V, Verner G, Kaback HR, and Iwata S (2003) Structure and mechanism of the lactose permease of *Escherichia coli*. *Science* **301:**610–615.

Arndt P, Volk C, Gorboulev V, Budiman T, Popp C, Ulzheimer-Teuber I, Akhoundova A, Koppatz S, Bamberg E, Nagel G, et al. (2001) Interaction of cations, anions, and weak base quinine with rat renal cation transporter rOCT2 compared with rOCT1. *Am J Physiol Renal Physiol* **281:**F454–F468.

Ermolova N, Madhvani RV, and Kaback HR (2006) Site-directed alkylation of cysteine replacements in the lactose permease of *Escherichia coli*: helices I, III, VI, and XI. *Biochemistry* **45:**4182–4189.

Gorboulev V, Shatskaya N, Volk C, and Koepsell H (2005) Subtype-specific affinity for corticosterone of rat organic cation transporters rOCT1 and rOCT2 depends on three amino acids within the substrate binding region. *Mol Pharmacol* **67:**1612–1619.

Gorboulev V, Volk C, Arndt P, Akhoundova A, and Koepsell H (1999) Selectivity of the polyspecific cation transporter rOCT1 is changed by mutation of aspartate 475 to glutamate. *Mol Pharmacol* **56:**1254–1261.

Gorbunov D, Gorboulev V, Shatskaya N, Mueller T, Bamberg E, Friedrich T, and Koepsell H (2008) High-affinity cation binding to organic cation transporter 1 induces movement of helix 11 and blocks transport after mutations in a modeled interaction domain between two helices. *Mol Pharmacol* **73:**50–61.

Ho SN, Hunt HD, Horton RM, Pullen JK, and Pease LR (1989) Site-directed mutagenesis by overlap extension using the polymerase chain reaction. *Gene* **77:**51–59.

Holyoake J and Sansom MSP (2007) Conformational change in an MFS protein: MD simulations of LacY. *Structure* **15:**873–884.

Kaback HR, Dunten R, Frillingos S, Venkatesan P, Kwaw I, Zhang W, and Ermolova N (2007) Site-directed alkylation and the alternating access model for LacY. *Proc Natl Acad Sci U S A* **104:**491–494.

Koepsell H, Lips K, and Volk C (2007) Polyspecific organic cation transporters: structure, function, physiological roles, and biopharmaceutical implications. *Pharm Res* **24:**1227–1251.

Lips KS, Volk C, Schmitt BM, Pfeil U, Arndt P, Miska D, Ermert L, Kummer W, and Koepsell H (2005) Polyspecific cation transporters mediate luminal release of acetylcholine from bronchial epithelium. *Am J Respir Cell Mol Biol* **33:**79–88.

Majumdar DS, Smirnova I, Kasho V, Nir E, Kong X, Weiss S, and Kaback HR (2007) Single-molecule FRET reveals sugar-induced conformational dynamics in LacY. *Proc Natl Acad Sci U S A* **104:**12640–12645.

Mehrens T, Lelleck S, Cetinkaya I, Knollmann M, Hohage H, Gorboulev V, Bokník P, Koepsell H, and Schlatter E (2000) The affinity of the organic cation transporter rOCT1 is increased by protein kinase C-dependent phosphorylation. *J Am Soc Nephrol* **11:**1216–1224.

Minuesa G, Volk C, Molina-Arcas M, Gorboulev V, Erkizia I, Arndt P, Clotet B, Pastor-Anglada M, Koepsell H, and Martinez-Picado J (2009) Transport of lamivudine [(−)-β-L-2′,3′-dideoxy-3′-thiacytidine] and high-affinity interaction of nucleoside reverse transcriptase inhibitors with human organic cation transporters 1, 2, and 3. *J Pharmacol Exp Ther* **329:**252–261.

Nagel G, Volk C, Friedrich T, Ulzheimer JC, Bamberg E, and Koepsell H (1997) A reevaluation of substrate specificity of the rat cation transporter rOCT1. *J Biol Chem* **272:**31953–31956.

Popp C, Gorboulev V, Müller TD, Gorbunov D, Shatskaya N, and Koepsell H (2005) Amino acids critical for substrate affinity of rat organic cation transporter 1 line the substrate binding region in a model derived from the tertiary structure of lactose permease. *Mol Pharmacol* **67:**1600–1611.

Rarey M, Kramer B, and Lengauer T (1999) The particle concept: placing discrete water molecules during protein-ligand docking predictions. *Proteins* **34:**17–28.

Rarey M, Kramer B, Lengauer T, and Klebe G (1996) A fast flexible docking method using an incremental construction algorithm. *J Mol Biol* **261:**470–489.

Reitman ML and Schadt EE (2007) Pharmacogenetics of metformin response: a step in the path toward personalized medicine. *J Clin Invest* **117:**1226–1229.

Schmitt BM, Gorbunov D, Schlachtbauer P, Egenberger B, Gorboulev V, Wischmeyer E, Müller T, and Koepsell H (2009) Charge-to-substrate ratio during organic cation uptake by rat OCT2 is voltage dependent and altered by exchange of glutamate 448 by glutamine. *Am J Physiol Renal Physiol* **296:**F709–F722.

Smirnova I, Kasho V, Choe JY, Altenbach C, Hubbell WL, and Kaback HR (2007) Sugar binding induces an outward facing conformation of LacY. *Proc Natl Acad Sci U S A* **104:**16504–16509.

Smirnova IN, Kasho VN, and Kaback HR (2006) Direct sugar binding to LacY measured by resonance energy transfer. *Biochemistry* **45:**15279–15287.

Sturm A, Gorboulev V, Gorbunov D, Keller T, Volk C, Schmitt BM, Schlachtbauer P, Ciarimboli G, and Koepsell H (2007) Identification of cysteines in rat organic cation transporters rOCT1 (C322, C451) and rOCT2 (C451) critical for transport activity and substrate affinity. *Am J Physiol Renal Physiol* **293:**F767–F779.

Volk C, Gorboulev V, Budiman T, Nagel G, and Koepsell H (2003) Different affinities of inhibitors to the outwardly and inwardly directed substrate binding site of organic cation transporter 2. *Mol Pharmacol* **64:**1037–1047.

Address correspondence to: Hermann Koepsell, Institute of Anatomy and Cell Biology, Koellikerstr. 6, 97070 Würzburg, Germany. E-mail: hermann@koepsell.de